Chapter 16

Automatic Optical Inspection of Soldering

Mihály Janóczki, Ákos Becker, László Jakab,
Richárd Gróf and Tibor Takács

Additional information is available at the end of the chapter

http://dx.doi.org/10.5772/51699

1. Introduction

Automatic Optical Inspection (AOI) or Automated Visual Inspection (AVI) is a control process. It evaluates the quality of manufactured products with the help of visual information. Amongst its several uses, one is the inspection of PWB (Printed Wiring Boards) after their assembling sequences i.e. paste printing, component placement and soldering. Nowadays, surface mount technology is the main method of assembly. It can be automated with ease. The increasing widespread use of SMT (Surface Mount Technology) in PWB assembly results in down-scaling of component size, increasing of lead count and component density. Parallel to this the latest manufacturing assembly lines have a very high rate of productivity. Not only is productivity required but a high quality also is expected. The quality requirements for electronic devices have already been standardized, e.g. IPC, ANSI-JSTD standards. Modern machines used in manufacturing lines such as paste printers, component placement machines etc. are capable of producing significantly better results than those required in normal standards specifications. Nowadays, the capability of modern manufacturing machines now reaches 6 σ as usually applied specification norm and 5 σ for more stringent ones. Even so, manufacturing processes are still kept under constant supervision. There still occasions when even a modern assembly line fails to create fully operational devices.

Besides the "classic" electric tests, such as in-circuit-test (ICT) and/or functional tests, there are in-line inspection possibilities: automatic optical inspection and automatic X-ray inspection systems. Because of their capabilities and properties, mostly the AOI systems are used as in-line quality inspection appliances. The main advantage of these systems is their ability to detect failures earlier and not only when the product has been assembled. AOI systems can be used to inspect the quality at each stage of the manufacturing process of the electronic device. Accordingly, there are real financial advantages by using such systems because the sooner a

INTECH
open science | open minds

© 2013 Janóczki et al.; licensee InTech. This is an open access article distributed under the terms of the Creative Commons Attribution License (http://creativecommons.org/licenses/by/3.0), which permits unrestricted use, distribution, and reproduction in any medium, provided the original work is properly cited.

failure can be detected, the smaller the likelihood of refuse device manufacturing. Because of component down-scaling and increasing in density, optical inspection is now only possible with the help of machine vision as opposed to manual inspection.

2. Rise of the AOI systems

Manufacturing electronic devices necessitates the constant controlling and inspection of the product. Previously, ICT was the main appliance used for this purpose. It inspected electronic components (e.g. resistor, capacitor etc.), checked for shorts, opens, resistance, capacitance and other basic quantities. Finally, it checked the proper operation of the whole circuit to show whether the assembly had been correctly fabricated. It operated by using a bed of measure-nails type test fixtures, designed for the current PWB and other specialist test equipment. It had the following disadvantages. As the dimensions of components were shrinking and the emplacement density was increasing, the positioning of the test-points became increasingly difficult. Beds of measure-nails are also relatively expensive and they are PWB-specific. This problem was however, partially solved by using flying-probe ICT systems (but at the expense of speed). Another disadvantage of ICT was that only finished product could be examined. It was able to detect failures but not to prevent them. It is also was not suitable for inspecting the quality of various assembling technologies. A further disadvantage was also in the case of functional testing. Extra measurement procedures had to be developed to ensure the enhancement of the quality of the manufacturing process.

Previously, the quality of solder joints had only been verified by manual visual inspection (MVI). The disadvantage of manual inspection, which at best was subjective, was that the tolerance limits were narrower than used in automated machines. A magnifying glass could help for a while, but as the mounting number of components per unit area exceeded the capabilities of manual testing, this option was already proving to be difficult or not even applicable as described in [1]. Because of the rapid development of digital computing, machine vision and image processing, it was obvious that it was becoming necessary to automate the process with the help of various high-resolution cameras, novel lighting devices [2], illumination techniques [3]-[5] and efficient image processing algorithms. Such state-of-the-art devices and solutions are described in detail in the following books: [6]-[8].

In cases where the manufacturing of large quantities of precise and high quality products takes place, the capabilities of production appliances can only be used effectively if the inspections, after various technological sequences are automated (in-line), are fast and reliable. As a result, the automatic optical inspection or testing appliances has been developed to replace manual inspection. The words, Automated Optical Inspection imply that when used in the manufacturing and assembly of PWBs, the nature of the inspection process itself, using digital machine vision and image processing, will give objective results.

AOI inspects bare and mounted PWBs automatically and uses optical information. It is faster, more accurate and cheaper than manual inspection. In preparing the parameters for such

http://dx.doi.org/10.5772/51699

inspections, parametric test procedures can be used to evaluate the digital image and on the basis of this they classify the inspected PWB, component or solder joint. Automatic Optical Inspection systems offer a reliable, flexible, fast and cost-effective solution when inspecting each step of the manufacturing process. Using AOI systems also has financial advantages. Detailed calculations show this in [1]. Further works give more reasons why AOI should be used. Several economic, efficiency and suitability studies have been undertaken about these systems [9]-[29].

3. Sensors, image capturing methods, structure

In the early 1970s, CCD (Charge Coupled Device) and CMOS (Complementary Metal–Oxide–Semiconductor) sensors were invented. It presented an opportunity to capture digital images that could be processed and evaluated by a computer. Machine vision was born. The subsequent exponential development resulted in an infinite number of these applications. One such development was the automatic optical inspection. Comparison between these sensors is reported in detailed [30]-[36].

Two kinds of methods exist to capture the images: FOI (Field of Interest) based matrix camera and line scan camera. The first captures several images on an optimized course, the second scans the whole surface of PWB. Both have their advantages and disadvantages. Line-scan is the faster method but the design of a proper source of illumination is more difficult or sometimes not possible at all because the position of components themselves affects the efficiency of illumination. If the component is parallel or perpendicular to the scanning line, the captured image could differ. In case of paste inspection, component positioning is out of question, so line-scan is better choice. For components and meniscus inspection, FOI is better. A new FOI generation method is shown in [37].

Basically AOI systems have three main parts: optical unit (illumination, cameras), positioning mechanism, and control system (Fig. 1).

4. Identifying PWB

AOI appliances identify the PWBs with the help of a separate built-in unit i.e. laser-scanner or by using its inbuilt functionality. On this basis, machines can decide what inspection is necessary. According to data contained in a barcode, the AOI system loads the appropriate inspection program. As barcodes (Fig. 2.a) became more widely used, in some cases the amount of data that could be stored in them was too limited and this became a barrier to its applicability. To solve this problem, the so-called ‘matrix codes’ (Fig. 2.b) were developed. In [30] 22 types of linear barcodes and 48 types of matrix codes are described.

Figure 1. The three main part of an AOI system

Figure 2. Example for: a) linear barcode b) DMC

5. Inspection of bare PWBs

There are several possibilities, appliances and algorithms when inspecting bare PWBs optically. These are able to inspect the copper wire-patterns on a PWB surface with high precision. Optical inspection gives rapid and reliable results regarding the quality of the PWB. Electrical detection methods, (e.g. ICT, Flying Probes) are slower and more expensive. Bare PWB inspecting AOIs have a special name: Automatic Optical Test (AOT) systems. There are several research and survey papers about this topic [31]-[43] and two manufacturers now have AOT machines [44]-[49]. In Table I a comparison between these appliances is shown.

http://dx.doi.org/10.5772/51699

Manufacturer	Amistar Automation Inc.	Lloyd Doyle Limited				
Model	K5L	doutech	Excalibur	phasor	redline	LD 6000
Board size max. [mm x mm]	510 x 410	610 x 760	610 x 760	760 x 760 (extended: 1000 x 2000)	610 x 760	610 x 760 (extended: 915 x 1525)
Board size min. [mm x mm]	50 x 50	n.a.	n.a.	n.a.	n.a.	n.a.
Board thickness [mm]	0.5 - 3.0	n.a.	n.a.	n.a.	n.a.	n.a.
Board warp [mm]	+ 0.5; - 1.0	n.a.	n.a.	n.a.	n.a.	n.a.
Board clearance top [mm]	50	n.a.	n.a.	n.a.	n.a.	n.a.
Board clearance bottom [mm]	50	n.a.	n.a.	n.a.	n.a.	n.a.
Camera type	CCD	n.a.	n.a.	n.a.	n.a.	n.a.
Illumination	3-stage LED dome lighting (Upper: IR; Middle: WH; Lower: WH)	n.a.	n.a.	n.a.	n.a.	n.a.
View size [mm]	30.4 x 22.8	500 x 635	500 x 610	500 x 635 (extended: 915 x 1980)	500 x 635 (extended: 1000 x 2000)	500 x 610 (extended: 865 x 1475)
Resolution [µm]	19	50	50	60	50	n.a.
Inspection time	0.45 sec/screen	20 - 60 sq. m/h	45 sq. m/h	n.a.	20 - 60 sq. m/h	15 sec @ 3/3 mil line/space; 27 sec @ 2/2 mil line/space (for 480 x 600 mm board size)
Applicability	missing components, position shift, rotation error, wrong components, polarity check, bridge, character recognition	functional and cosmetic faults	functional and cosmetic faults	functional and cosmetic faults	functional and cosmetic faults	functional and cosmetic faults

Table 1. Comparison of Automatic Optical Test (AOT) machines

6. Inspections following SMT sequences

In the SMT assembling process there are three main phases where AOI plays an important role; after-paste printing, component placement and soldering. In the case of wave, r selective or partial soldering there are other sequences e.g. glue dispensing, through-hole component insertion etc. But SMT processes are used mainly for inspection in discussions about this method of assembly. Possible locations where AOI can be placed in an SMT line are: the post-paste, post-placement or pre-reflow and post reflow (Fig. 3.).

At each location AOI appliances have a special name. These are: Solder Paste Inspection (SPI, also known as Post-Printing Inspection), Automatic Placement Inspection (API. also known as Post-Placement Inspection) and Post-Soldering Inspection (PSI). The AOI systems able to inspect each manufacturing sequence are called: Universal AOI (UAOI). If there is a possibility that the equipment can inspect the finished product optically, it is then called the Automatic Final Inspection (AFI).

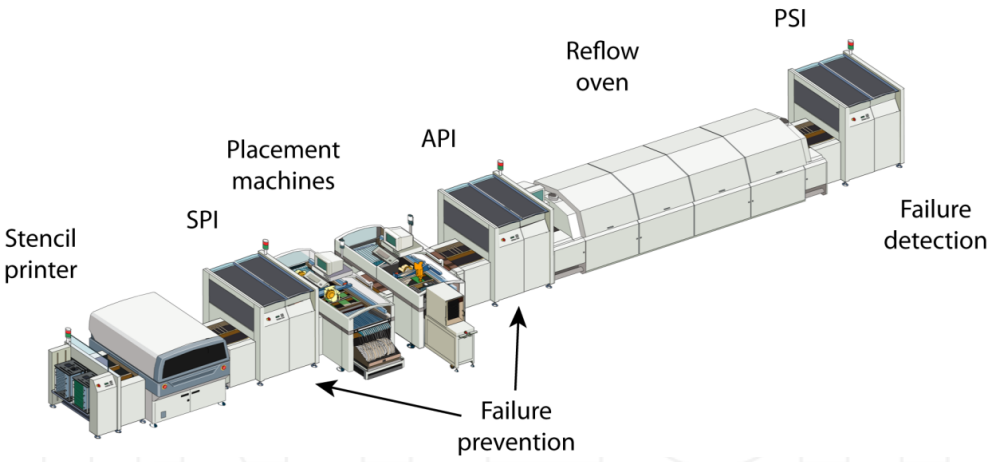

Figure 3. Possible places of AOI systems

6.1. Solder paste inspection

According to PWB assemblers, it is very important that the quality of the print solder paste is inspected because it heavily influences the quality of solder joints. In some papers it has been reported that 52%–71% of SMT defects are related to the printing process [50]-[53]. As failures can be detected much earlier, this obviously results in cost savings. According to some other opinions, inspection of the solder paste is not so relevant: "Contrary to the common, frequently quoted opinion that paste faults represent the primary percentage or 70% of all faults in the printed circuit assembly process, this detailed analysis shows that those faults amounted to only 8.3%." [54].

Special AOI machines are able to inspect the quality of print of the solder paste. It is an important option because in case of failure, the product can be repaired with minimum cost and without scrap loss. The size of the print in the 3 dimensions examined (latitude, longitude, altitude) must fall within the limits specified. To measure these parameters, so-called SPI (Solder Paste Inspection) machines have been developed. These machines are able to inspect only one step i.e. paste printing, but they are cheaper than universal AOI machines. As the control of solder paste presence is one of the easier tasks, then only the width, length and position needs to be inspected and so several failures can be detected such as bridges [55]. This can be solved using image capturing (usually with the help of line scan cameras) and subsequent evaluation.

But to measure volume as well the paste thickness is equally as important. Comparison between 2D and 3D solder paste inspections are reported in [56] and [57]. There are several possibilities to enable the measurement of paste volume optically: laser scanner [58]-[63]; projected sinusoidal fringe pattern as in [64]; the development of this technique for solder paste geometry measurement in [65], [66] and some special methods shown in [67]-[69]. Nine manufacturers offer SPI systems [70]-[82]. Several different solutions have been developed in these appliances as can be found in the scientific literature, described above. Comparison between the different methods is shown in Table 2.

http://dx.doi.org/10.5772/51699

Manufacturer	Model	Board size max. [mm x mm]	Board size min. [mm x mm]	Maximum board weight [kg]	Maximum inspection area [mm]	Maximum pad size in field of view [mm]	Typical inspection speed @ high speed [sq. cm/sec]	Typical inspection speed @ high resolution [sq. cm/sec]	Typical inspection speed @ unload and fiducial find [sec]	X and Y pixel size @ high speed [µm]	X and Y pixel size @ high resolution [µm]	Paste height range [µm]	Height resolution [µm]	Measurement types
CyberOptics	SE 300 Ultra	508 x 508	101 x 40	3	508 x 503	5 x 10	29.0	16.0	3 - 4	40	20	50 - 610	0.13	height, area, volume, registration, bridge detection
CyberOptics	SE 500	510 x 510	50 x 50	3 - 5	508 x 503	15 x 15	80.0	50.0	4 - 5	30	15	50 - 500	0.20	height, area, volume, registration, bridge detection
CyberOptics	SE 500-X	810 x 610	100 x 100	10	810 x 605	15 x 15	80.0	50.0	4 - 5	30	15	50 - 500	0.20	height, area, volume, registration, bridge detection
Koh Young Technology	aSPIre	n.a.	n.a.	n.a.	n.a.	n.a.	41.0	n.a.	n.a.	10	20	20 - 400	0.37	height, area, volume, offset, bridge detection, shape deformity
Koh Young Technology	KY-8030	n.a.	n.a.	n.a.	n.a.	n.a.	15.0	19.7	n.a.	20	20	20 - 400	0.37	height, area, volume, offset, bridge detection, shape deformity
Marantz	Power Spector	510 x 460	50 x 50	n.a.	n.a.	n.a.	80.0	80.0	n.a.	n.a.	n.a.	max. 600	n.a.	height, area, volume, offset, bridge detection, shape deformity
Omron	VT-RNS-P	510 x 460	50 x 50	n.a.	n.a.	n.a.	n.a.	n.a.	n.a.	10; 15; 20	10; 15; 20	n.a.	n.a.	presence of solder, insufficient solder, excessive solder, solder shifting, grazing, bridging, spreading
Omron - CKD	VP5000L	510 x 460	50 x 50	n.a.	n.a.	n.a.	n.a.	n.a.	n.a.	12	12	n.a.	n.a.	average height, volume, excessive deposition, insufficient solder, smearing, misalignment, bridging
Orpro Vision	Symbian P36	508 x 540	n.a.	n.a.	n.a.	n.a.	60	60	4 - 6	20	20	50 - 300	5.00	n.a.
Saki	BF-SPIder-M	250 x 330	50 x 60	n.a.	n.a.	n.a.	n.a.	n.a.	3	12	12	max. 450	0.40	height, area, volume, shift, shape, spread, bridge
Saki	BF-SPIder-L	460 x 500	50 x 60	n.a.	n.a.	n.a.	n.a.	n.a.	3 - 5	12	12	max. 450	0.40	height, area, volume, shift, shape, spread, bridge
ScanCAD	ScanINSPECT SPI	457 x 508	50 x 50	n.a.	419 x 508	n.a.	n.a.	n.a.	n.a.	n.a.	n.a.	n.a.	n.a.	n.a.
TRI Innovation	TR7006/L/LL-20	330 x 280	50 x 50	3	n.a.	n.a.	98.8	24.7	n.a.	20	20	40 - 600	n.a.	n.a.
TRI Innovation	TR7006/L/LL-16	510 x 460	50 x 50	5	n.a.	n.a.	63.2	15.8	n.a.	16	16	32 - 480	n.a.	n.a.
TRI Innovation	TR7006/L/LL-12	660 x 610	50 x 50	10	n.a.	n.a.	35.5	8.8	n.a.	12	12	24 - 360	n.a.	n.a.
TRI Innovation	TR7066-20	510 x 460	50 x 50	3	n.a.	n.a.	153.6	23.0	n.a.	20	20	40 - 600	n.a.	n.a.
TRI Innovation	TR7066-16	510 x 460	50 x 50	3	n.a.	n.a.	122.9	18.4	n.a.	16	16	32 - 480	n.a.	n.a.
TRI Innovation	TR7066-12	510 x 460	50 x 50	3	n.a.	n.a.	92.2	13.8	n.a.	12	12	24 - 360	n.a.	n.a.
Viscom	S3088-II QS	450 x 350	n.a.	n.a.	n.a.	n.a.	110	110	n.a.	22	22	n.a.	n.a.	n.a.
Vi Technology	3D-SPI	510 x 460	n.a.	n.a.	n.a.	n.a.	20.0	20.0	n.a.	n.a.	n.a.	n.a.	n.a.	height, area, volume, bridge, shape, position

Table 2.

Manufacturer	Model	Conveyor speed [mm/sec]	Conveyor height [mm]	Board warp	Volume repeatability on a certification target	Volume repeatability on a circuit board	Gage R&R	Measurement types
CyberOptics	SE 300 Ultra	150 - 450	889 - 990	<2% of PCB diagonal or 6.35mm total	n.a.	n.a.	n.a.	height, area, volume, registration, bridge detection
CyberOptics	SE 500	150 - 450	810 - 970	<2% of PCB diagonal or 6.35mm total	< 1%; 3 σ	<3%; 3 σ	<< 10%; 6 σ	height, area, volume, registration, bridge detection
CyberOptics	SE 500-X	150 - 450	810 - 970	<2% of PCB diagonal or 6.35mm total	< 1%; 3 σ	<3%; 3 σ	<< 10%; 6 σ	height, area, volume, registration, bridge detection
Koh Young Technology	aSPIre	n.a.	830 - 970	± 5.0 mm	< 1%; 3 σ	<3%; 3 σ	<< 10%; 6 σ	height, area, volume, offset, bridge detection, shape deformity
Koh Young Technology	KY-8030	n.a.	870 - 970	± 3.5 mm	< 1%; 3 σ	<3%; 3 σ	<< 10%; 6 σ	height, area, volume, offset, bridge detection, shape deformity
Marantz	Power Spector	n.a.	830 - 970	± 5.0 mm	n.a.	n.a.	n.a.	height, area, volume, offset, bridge detection, shape deformity
Omron	VT-RNS-P	n.a.	n.a.	n.a.	n.a.	n.a.	n.a.	presence of solder, insufficient solder, excessive solder, solder shifting, grazing, bridging, spreading
Omron - CKD	VP5000L	n.a.	n.a.	n.a.	n.a.	n.a.	n.a.	average height, volume, excessive deposition, insufficient solder, smearing, misalignment, bridging
Orpro Vision	Symbion P36	n.a.	870 - 930	+ 3.0 mm; - 6.0 mm	n.a.	n.a.	< 10%	n.a.
Saki	BF-SPIder-M	n.a.	max. 900	n.a.	< 1%; 3 σ	n.a.	< 10%	height, area, volume, shift, shape, spread, bridge
Saki	BF-SPIder-L	n.a.	max. 900	n.a.	< 1%; 3 σ	n.a.	< 10%	height, area, volume, shift, shape, spread, bridge
ScanCAD	ScanINSPECT SPI	n.a.	n.a.	n.a.	n.a.	n.a.	n.a.	n.a.
TRI Innovation	TR7006/L/LL-20	n.a.	n.a.	n.a.	n.a.	n.a.	n.a.	n.a.
TRI Innovation	TR7006/L/LL-16	n.a.	n.a.	n.a.	n.a.	n.a.	n.a.	n.a.
TRI Innovation	TR7006/L/LL-12	n.a.	n.a.	n.a.	n.a.	n.a.	n.a.	n.a.
TRI Innovation	TR7066-20	n.a.	n.a.	n.a.	n.a.	n.a.	n.a.	n.a.
TRI Innovation	TR7066-16	n.a.	n.a.	n.a.	n.a.	n.a.	n.a.	n.a.
TRI Innovation	TR7066-12	n.a.	n.a.	n.a.	n.a.	n.a.	n.a.	n.a.
Viscom	S3088-II QS	n.a.	850 - 960	n.a.	n.a.	n.a.	n.a.	n.a.
Vi Technology	3D-SPI	n.a.	max. 950	± 3.5 mm	n.a.	n.a.	< 10%	height, area, volume, bridge, shape, position

Table 3. Comparison of Solder Paste Inspection (SPI) machines

6.2 Automatic placement inspection

Inspection of the PWB after component placement is the next possibility. With this method possible placement failures can be detected and some defective paste printing phenomena as well. If there is a sign or mark on the component, it can be read and identified with the help of modern image processing algorithms even if it has more than one different-looking label type. APIs (Table III) are able to measure most parameters of components objectively e.g. X-Y shift, rotation, polarity, labels, size etc. [83]-[90]. Four manufacturers have this special appliance in stock. [91]-[94].

Manufacturer	BeamWorks	Landrex	Omron	Viscom
Model	Inspector cpv	Optima II 7301 Express	VT-RNS-Z	S3054QV
Field of view	12 x 9 mm @ 15 µm; 48 x 36 mm @ 73 µm	10 x 10 mm; 15 x 15 mm	n.a.	1280 x 1024 pixel
Pixel size [µm]	15; 73	n.a.	10; 15; 20	10; 22
Depth of field (max. component height for inspection) [mm]	10; 15	n.a.	n.a.	n.a.
Number of cameras	1	1 vertical, 4 angled	1	1
Lighting method	oblique ring, white LED light	n.a.	ring-shaped RGB LED	n.a.
Board size max. @ single board operation [mm x mm]	508 x 406	609 x 558	510 x 460	443 x 406
Board size max. @ dual board operation [mm x mm]	none	none	none	370 x 406
Board size min. [mm]	40 x 28	51 x 76	50 x 50	n.a.
Board thickness [mm]	0.8 - 3.2	n.a.	n.a.	n.a.
Conveyor height [mm]	n.a.	n.a.	n.a.	850 - 960
Board edge clearance [mm]	4	n.a.	n.a.	3
Board edge clearance top [mm]	25; 37	63	20	35
Board edge clearance bottom [mm]	25; 37	63	50	50
Inspection speed [sq. cm/sec]	2 @ 12 x 9 mm field of view	n.a.	250 ms/screen @ 10 sq. mm field of view	20 - 30
Applicability	missing component, wrong component, polarity check, offset, skew	missing components, misoriented components, extra components, component placement, tombstoned and bill boarded components, lifted leads, insufficient solder and excess solder, wrong part, through hole pins	presence of solder, component shifting, polarity error, missing components, wrong components, solder balls, skewing, bridging, foreign objects	n.a.

Table 4. Comparison of Automatic Placement Inspection (API) machines

6.3 Post soldering inspection

Most manufacturers agree from a strategic point of view, that optical inspection after soldering has been completed should not be missed out. At the very least, the defective products must be eliminated because many failures are generated during soldering: “Forty-nine percent of the true faults were detectable only after soldering. These consisted of component and soldering faults. Forty-eight percent of the optically recognizable faults could not be recognized electrically.” [54].

In consequence, this is the most important part of the AOI inspection process. Most scientific papers are preoccupied with this subject [95]-[123]. The quality of the solder joint (and the soldering process) can be inspected with the methods described in this section. The quality of the solder joints is determined from geometric and optical properties of the solder meniscus. These parameters determine the reflection properties of the meniscus which is formed from the liquid alloy during the soldering process. After cooling, the meniscus becomes solid and reflects illumination which means that we can evaluate it (Fig.5, Fig. 6). From these reflection patterns and with the help of image processing algorithms we are able to determine the quality of the solder joints.

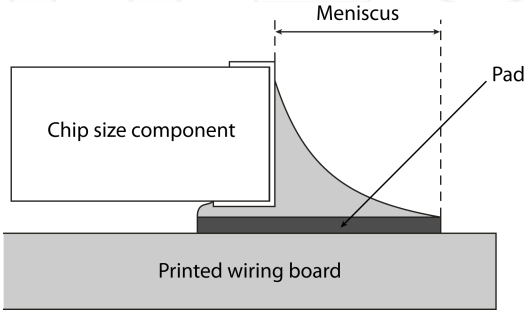

Figure 4. Schematic of the meniscus

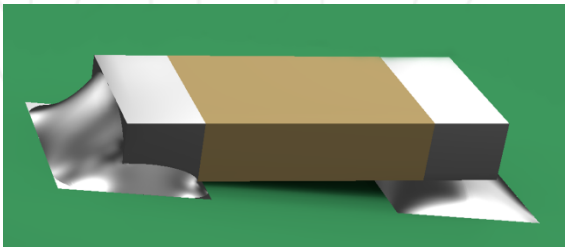

Figure 5. Reflection pattern on meniscus model with white ring illumination

http://dx.doi.org/10.5772/51699

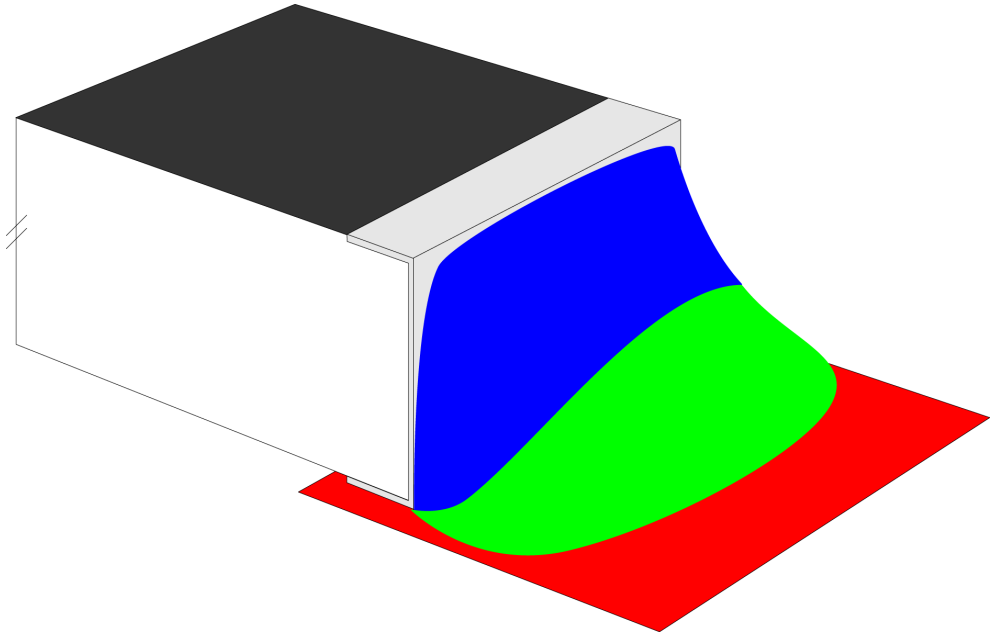

Figure 6. Reflection pattern on meniscus model with RGB ring illumination

Using reflection patterns is the basis of all papers that have been published in this field of study. There are two solutions: gray-scale or colour inspection. Supplier and appliances are shown in Table IV [124]-[126].

One interesting area is wave soldering. It needs different types of algorithms because of the circular solder shape and the pin. Some solutions for this kind of inspection are reported in [127]-[129]. A summary of possible failures and appliances that can detect them are shown in Table V.

6.4. Combined appliances

There are systems that are able to inspect more sequences. These are combined systems, namely API&PSI [140]-[146] (Table VI).

And the all-in-one machines are the UAOI systems, detailed: SPI&API&PSI [147]-[163] (Table VII).

Manufacturer	TRI Innovation	Viscom	
Model	TR7530	S3016	S3054QC
Field of view (orthogonal camera) [pixel]	1024 x 768	2752 x 2048 @ 55 x 43 mm	672 x 512
Pixel size (orthogonal camera) [µm]	10; 15; 20	22; 10	22; 10
Number of cameras (orthogonal)	1	4	1, 2 or 4
Resolution (angled view camera) [µm/pixel]	n.a.	15	n.a.
Number of cameras (angled view)	n.a.	4	n.a.
Illumination	ultra-low angle, multi-segment, RGB LED lighting	n.a.	n.a.
Inspection speed	72 sq. cm/sec @ 20 µm; 40 sq. cm/sec @ 10 µm; 18 sq. cm/sec @ 10 µm	typical connector with 100 pins 15 sec	typical connector with 100 pins 15 sec
Board size max. [mm]	400 x 300	430 x 406	443 x 406
Board size min. [mm]	50 x 50	n.a.	n.a.
Board weight max. [kg]	3	n.a.	n.a.
Conveyor height [mm]	n.a.	850 - 960	850 - 960
Board edge clearance [mm]	3	3	3
Board clearance top [mm]	25	50	15
Board clearance bottom [mm]	40	35	50
Applicability	missing component, tombstone, billboard, polarity, skew, marking, defective, insufficient and excess solder, bridge, trough hole pin, lifted lead, golden finger, scratch, blur	selective and special solder joints	selective and special solder joints

Table 5. Comparison of Post Soldering Inspection (PSI) machines

http://dx.doi.org/10.5772/51699

	UAOI					
	SPI	API	PSI		API	PSI
	paste inspection	pre reflow component in paste	post reflow	adhesive inspection	pre wave component in adhesive	post wave
missing paste	✓	✓				
completeness or/and volume of solder paste	✓	✓ whether it is not covered by component				
misalignment	✓					
paste bridge	✓	✓				
smeared solder paste	✓	✓ whether it is not covered by component				
contamination	✓	✓ whether it is not covered by component	✓		✓	✓
missing component		✓	✓		✓	✓
component position (x-y shift, rotation, face lift)		✓	✓		✓	✓
polarity		✓	✓		✓	✓
damaged component		✓	✓		✓	✓
unsoldered component			✓			✓
insufficient solder joint			✓			✓
solder bridge			✓			✓
lifted lead			✓			✓
tombstone			✓			✓
missing adhesive				✓		
smeared adhesive on pad				✓		
missing pin end						✓
insufficient pin solder						✓
dewetting						✓
PWB registration	✓	✓	✓	✓	✓	✓

Table 6. Possible failures and appliances

Manufacturer	Model	Camera movement	Board movement	Component inspection	Printing/paste inspection	Distinction principles	Distinction parameters	Camera type	Camera field of view/resolution	Lens	Illumination
Machine Vision Products	Supra E	n.a.	n.a.	n.a.	n.a.	n.a.	n.a.	5MP color camera	7 - 17 µm	n.a.	programmable variable LED strobe lighting, proprietary multi-color illumination
Marantz	iSpector HDL 350L	X + Y direction	stationary during inspection	presence, polarity, offset, correctness, soldering	offset, smearing, bridges, uniformity	synthetic imaging, spectral analysis, grayscale limits	brightness, hue, saturation via filters	UXGA CCD digital camera with CameraLink	32 x 24 mm @ 20 µm; 40 x 30 mm @ 25 µm; 16 x 12 mm @ 10 µm	telecentric lens with built in prism for DOAL lighting	omnidirectional triple LED rings; side, main, line sourced DOAL (diffused on axis lighting (coaxial))
Marantz	iSpector HDL 650L	X + Y direction	stationary during inspection	presence, polarity, offset, correctness, soldering	offset, smearing, bridges, uniformity	synthetic imaging, spectral analysis, grayscale limits	brightness, hue, saturation via filters	UXGA CCD digital camera with CameraLink	32 x 24 mm @ 20 µm; 40 x 30 mm @ 25 µm; 16 x 12 mm @ 10 µm	telecentric lens with built in prism for DOAL lighting	omnidirectional triple LED rings; side, main, line sourced DOAL (diffused on axis lighting (coaxial))
Marantz	iSpector HML 350L	X + Y direction	stationary during inspection	presence, polarity, offset, correctness, soldering	offset, smearing, bridges, uniformity	synthetic imaging, spectral analysis, grayscale limits	brightness, hue, saturation via filters	UXGA CCD digital camera with CameraLink	32 x 24 mm @ 20 µm; 40 x 30 mm @ 25 µm; 16 x 12 mm @ 10 µm	high resolution telecentric	omnidirectional 4-angle LED: RGB-DOAL (coaxial)
Marantz	iSpector HML 650L	X + Y direction	stationary during inspection	presence, polarity, offset, correctness, soldering	offset, smearing, bridges, uniformity	synthetic imaging, spectral analysis, grayscale limits	brightness, hue, saturation via filters	UXGA CCD digital camera with CameraLink	32 x 24 mm @ 20 µm; 40 x 30 mm @ 25 µm; 16 x 12 mm @ 10 µm	high resolution telecentric	omnidirectional 4-angle LED: RGB-DOAL (coaxial)
Orpro Vision	Symbion S36	stationary during inspection	X + Y + Z direction	presence and absence of components, placement accuracy and polarity, optical character recognition	insufficient solder, tombstone, billboard, coplanarity, lifted leads, shorts	n.a.	n.a.	4MP XGA high resolution top and 4 side cameras with symmetric image acquisition and color capability	n.a.	n.a.	axial, direct, diffuse and RGB multi-color illumination
TRI Innovation	7500	n.a.	n.a.	missing, tombstone, billboard, polarity, shift	insufficient solder, excess solder, bridge	n.a.	n.a.	1 top view XGA 3CCD camera @ 1024 x 768 pixel, 4 angle view XGA mono camera & 1024 x 768 pixel	10 µm; 15 µm; 20 µm; 25 µm	n.a.	multi segment, multi angle LED, RGB+W
TRI Innovation	7500L	n.a.	n.a.	missing, tombstone, billboard, polarity, shift	insufficient solder, excess solder, bridge	n.a.	n.a.	1 top view XGA 3CCD camera @ 1024 x 768 pixel, 4 angle view XGA mono camera & 1024 x 768 pixel	10 µm; 15 µm; 20 µm; 25 µm	n.a.	multi segment, multi angle LED, RGB+W
TRI Innovation	7550	n.a.	n.a.	missing, tombstone, billboard, polarity, skew, marking, defective	insufficient solder, excess solder, bridge, trough hole pins, lifted lead, golden finger scratch, blur	n.a.	n.a.	1 top view XGA 3CCD camera @ 1024 x 768 pixel, 4 angle view XGA mono camera & 1024 x 768 pixel	10 µm; 15 µm; 20 µm; 25 µm	n.a.	multi segment, multi angle LED, RGB (coaxial lighting optional)
Sony	SI-V200	n.a.	n.a.	inaccurate mounting, reversed, polarity	missing, solder, bridging, solder quantity	n.a.	n.a.	2MP color CCD camera	24.8 x 18.6 mm @ 15.5 µm; 17.6 x 13.2 mm @ 11 µm	n.a.	high intensity white LED
Saki	BF-Tristar	n.a.	n.a.	presence and absence of components, misalignment, tombstone, reverse, polarity, bridge, foreign material, lifted lead, lifted chip	absence, insufficient solder, fillet defect	n.a.	n.a.	line color CCD camera	10 µm	n.a.	LED lighting system

Table 7.

http://dx.doi.org/10.5772/51699

Manufacturer	Model	Minimum inspection component size	Position accuracy	Board clearance top [mm]	Board clearance bottom [mm]	Board size max. [mm x mm]	Board size min. [mm x mm]	Movement speed [mm/sec]	Inspection capacity typical	Conveyor speed [mm/sec]	Conveyor height [mm]	Board clamping	Board thickness [mm]
Machine Vision Products	Supra E	0201 and 01005 (0.4 x 0.2 mm)	0.5 µm	n.a.	n.a.	508 x 508	n.a.	n.a.	90 sq. cm/sec	n.a.	n.a.	n.a.	n.a.
Marantz	iSpector HDL 350L	01005 (0.4 x 0.2 mm @ 10 µm)	pixel related feedback loop	40	35, 55	350 x 250	50 x 50	720	1500 cps/min	10 - 500	830 - 950	ruler blade, top & edge clamping, sensor stopper	0.6 - 4.0
Marantz	iSpector HDL 650L	01005 (0.4 x 0.2 mm @ 10 µm)	pixel related feedback loop	40	35, 55	650 x 550	50 x 50	720	1500 cps/min	10 - 500	830 - 950	ruler blade, top & edge clamping, sensor stopper	0.6 - 4.0
Marantz	iSpector HML 350L	01005 (0.4 x 0.2 mm @ 10 µm)	pixel related feedback loop	30	35, 55	350 x 250	50 x 50	720	1500 cps/min	10 - 500	n.a.	ruler blade, top & edge clamping, sensor stopper	0.6 - 4.0
Marantz	iSpector HML 650L	01005 (0.4 x 0.2 mm @ 10 µm)	pixel related feedback loop	30	35, 55	650 x 550	50 x 50	720	1500 cps/min	10 - 500	n.a.	ruler blade, top & edge clamping, sensor stopper	0.6 - 4.0
Orpro Vision	Symbion S36	01005 (0.4 x 0.2 mm) down to 0.3 mm pitch	n.a.	90	90	550 x 470	n.a.	n.a.	40 sq. cm/sec	n.a.	n.a.	n.a.	n.a.
TRI Innovation	7500	n.a.	n.a.	50	50	510 x 460	n.a.	n.a.	110 sq. cm/sec @ 25 µm; 72 sq. cm/sec @ 20 µm; 40 sq. cm/sec @ 15 µm; 18 sq. cm/sec @ 10 µm;	n.a.	n.a.	n.a.	max. 4.0
TRI Innovation	7500L	n.a.	n.a.	50	50	660 x 610	n.a.	n.a.	110 sq. cm/sec @ 25 µm; 72 sq. cm/sec @ 20 µm; 40 sq. cm/sec @ 15 µm; 18 sq. cm/sec @ 10 µm;	n.a.	n.a.	n.a.	max. 4.0
TRI Innovation	7550	n.a.	n.a.	40	40	540 x 460	50 x 50	n.a.	110 sq. cm/sec @ 25 µm; 72 sq. cm/sec @ 20 µm; 40 sq. cm/sec @ 15 µm; 18 sq. cm/sec @ 10 µm;	n.a.	n.a.	n.a.	0.6 - 4.0
Sony	SI-V200	0402 @ high resolution, 0603 @ normal resolution	n.a.	20	40	460 x 510	40 x 50	n.a.	0,27 sec/frame	n.a.	n.a.	n.a.	0.4 - 2.0
Saki	BF-Tristar	n.a.	n.a.	30	30	250 x 330	50 x 70	n.a.	20 sec / 250 x 350 mm	n.a.	900	n.a.	0.6 - 2.5

Table 8. Comparison of combined (API&PSI) machines

Manufacturer	Model	Pre-reflow inspection	Post-reflow inspection	Camera type	Orthogonal camera field of view [mm]	Orthogonal camera resolution [µm]	Number of orthogonal cameras	Angular camera resolution [µm]	Number of angular cameras	Illumination
Agilent Technologies	Medalist SJ50 Series 3	missing, offset, 2D paste, skewed, polarity, bridging, wrong part, traceability	missing, offset, skewed, polarity, billboard, tombstone, lifted/bent leads, excess/insufficient solder, bridging, wrong part, traceability	4 megapixel digital camera	44.7 x 32.8	19; 12	n.a.	n.a.	n.a.	multiple color, multiple angle, multiple segment ED lighting head, auto-calibration
Agilent Technologies	Medalist SJ50 Series 3 XL	missing, offset, 2D paste, skewed, polarity, bridging, wrong part, traceability	missing, offset, skewed, polarity, billboard, tombstone, lifted/bent leads, excess/insufficient solder, bridging, wrong part, traceability	4 megapixel digital camera	44.7 x 32.8	19; 12	n.a.	n.a.	n.a.	multiple color, multiple angle, multiple segment ED lighting head, auto-calibration
Agilent Technologies	Medalist sj5000	missing, offset, 2D paste, skewed, polarity, bridging, billboard, wrong part , extra part, traceability	missing, offset, skewed, polarity, billboard, tombstone, lifted/bent leads, excess/insufficient solder, bridging, wrong part, traceability	4 megapixel digital camera	44.7 x 32.8	21; 12	n.a.	n.a.	n.a.	multiple color, multiple angle, multiple segment ED lighting head, auto-calibration
Amistar Automation Inc.	K2	position shift, blur, solder area, bridge	missing components, position shift, rotation error, wrong components, polarity check, bridge, character recognition, solder quantity, lifted leads	CCD	30.4 x 22.8	19	n.a.	n.a.	n.a.	auto-adjust 3-stage LED dome lighting (Upper: IR; Middle: WH; Lower: WH)
Amistar Automation Inc.	K2L	position shift, blur, solder area, bridge	missing components, position shift, rotation error, wrong components, polarity check, bridge, character recognition, solder quantity, lifted leads	CCD	30.4 x 22.8	19	n.a.	n.a.	n.a.	auto-adjust 3-stage LED dome lighting (Upper: IR; Middle: WH; Lower: WH)
CyberOptics	Flex HR 8	missing, polarity, billboard, flipped, wrong part, gross body and lead damage, gold-finger contamination,	missing, polarity, billboard, flipped, wrong part, gross body and lead damage, gold-finger contamination, tombstone, solder bridge, opens, lifted leads, wettability, excess/insufficient solder, debris	5 megapixel color CMOS camera	n.a.	17	5	n.a.	n.a.	fluorescent white light
CyberOptics	Flex HR 12	missing, polarity, billboard, flipped, wrong part, gross body and lead damage, gold-finger contamination,	missing, polarity, billboard, flipped, wrong part, gross body and lead damage, gold-finger contamination, tombstone, solder bridge, opens, lifted leads, wettability, excess/insufficient solder, debris	5 megapixel color CMOS camera	n.a.	17	8	n.a.	n.a.	fluorescent white light
CyberOptics	Flex HR 11	missing, polarity, billboard, flipped, wrong part, gross body and lead damage, gold-finger contamination,	missing, polarity, billboard, flipped, wrong part, gross body and lead damage, gold-finger contamination, tombstone, solder bridge, opens, lifted leads, wettability, excess/insufficient solder, debris	5 megapixel color CMOS camera	n.a.	17	11	n.a.	n.a.	fluorescent white light
Machine Vision Products	Ultra IV	n.a.	n.a.	n.a.	n.a.	8 - 17	n.a.	n.a.	n.a.	programmable variable LED strobe lighting, proprietary multi-color illumination
Mirtec	MV-7	n.a.	n.a.	1.3, 2 or 4 megapixel digital color camera	14.0 x 10.5 to 37.2 x 37.2	9.8 - 18.2	n.a.	n.a.	4	n.a.
Mirtec	MV-7L	n.a.	n.a.	1.3, 2 or 4 megapixel digital color camera	14.0 x 10.5 to 37.2 x 37.2	9.8 - 18.2	n.a.	n.a.	4	n.a.
Mirtec	MV-7xi	n.a.	n.a.	1.3, 2 or 4 megapixel digital color camera	14.0 x 10.5 to 37.2 x 37.2	9.8 - 18.2	n.a.	n.a.	4	n.a.
Mirtec	MV-7U	n.a.	n.a.	1.3, 2 or 4 megapixel digital color camera	14.0 x 10.5 to 37.2 x 37.2	9.8 - 18.2	n.a.	n.a.	4	n.a.
Omron	VT-RNS-S	presence of solder, wrong components, missing components, bridging, component shifting, lead bending	presence of solder, wrong components, missing components, bridging, tombstone, component shifting, fillet, wettability, lead bending, adhesive, solder balls	3-CCD camera	n.a.	10; 15; 20	n.a.	n.a.	n.a.	ring-shaped LED (red, green, blue)
Omron	VT-WIN II	presence/absence, skewed, shifted, wrong component, un-inserted, upside-down/backward, polarity, lead bent	presence/absence of solder, excessive solder, insufficient solder, blow holes, wettability, bridges, solder balls, skewed, shifted, wrong component, polarity, lead bent	triple element CCD camera	n.a.	10; 13; 15; 20; 25; 30; 35; 50	n.a.	n.a.	n.a.	3 ring-shaped LED arrays with automatic brightness control
Saki	BF-Frontier	presence/absence, misalignment, polarity, bridge	presence/absence, tombstone, reverse, polarity, bridge, foreign material, absence of solder, insufficient solder, lifted lead, lifted chip, fillet	line color CCD camera	n.a.	18	n.a.	n.a.	n.a.	LED lighting system
Saki	BF-Planet-X	presence/absence, misalignment, polarity, bridge	presence/absence, tombstone, reverse, polarity, bridge, foreign material, absence of solder, insufficient solder, lifted lead, lifted chip, fillet	line color CCD camera		10	n.a.	n.a.	n.a.	LED lighting system
Viscom	S3088-III	n.a.	n.a.	megapixel	57.6 x 43.5	23.4; 11.7	4	16.1; 8.05	4; 8	n.a.
Viscom	S3088-II	n.a.	n.a.	megapixel	57.6 x 43.5	23.4; 11.7	4	16.1; 8.05	4; 8	n.a.
Viscom	S6056-ST1	n.a.	n.a.	megapixel	57.6 x 43.5	23.4; 11.7	4	16.1; 8.05	4; 8	n.a.
Viscom	S6056-DS1W	n.a.	n.a.	megapixel	57.6 x 43.5	23.4; 11.7	4	16.1; 8.05	4; 8	n.a.
Viscom	S6056-DS2W	n.a.	n.a.	megapixel	57.6 x 43.5	23.4; 11.7	4	16.1; 8.05	4; 8	n.a.
Vi Technology	3K Series	n.a.	n.a.	1620 x 1220 pixel; 2352 x 1728 pixel	42.1 x 31.7; 61.1 x 44.9	8 - 12	n.a.	n.a.	n.a.	i-LITE (red, green, blue); axial and peripheral
Vi Technology	5K Series	n.a.	n.a.	1620 x 1220 pixel; 2352 x 1728 pixel	42.1 x 31.7; 61.1 x 44.9	8 - 12	n.a.	n.a.	n.a.	i-LITE (red, green, blue); axial and peripheral
Vi Technology	7K Series	n.a.	n.a.	1620 x 1220 pixel; 2352 x 1728 pixel	42.1 x 31.7; 61.1 x 44.9	8 - 12	n.a.	n.a.	n.a.	i-LITE (red, green, blue); axial and peripheral
Vi Technology	Vi-5000	n.a.	n.a.	1360 x 1040 pixel	44.5 x 33.6	12	n.a.	n.a.	n.a.	amber, green, blue
Vi Technology	Vi-5000-2	n.a.	n.a.	1600 x 1152 pixel	41.6 x 29.9	8	n.a.	n.a.	n.a.	green, white, blue, axial and peripheral
Vi Technology	Vi-5000-3	n.a.	n.a.	2048 x 2048 pixel	53.2 x 53.2	8	n.a.	n.a.	n.a.	green, white, blue
YES Tech	YTV-F1	position, missing, wrong, polarity, skew	polarity, skew, tombstone, bent lead, lifted, bridging, open solder, insufficient, short, solder balls	Multiple Thin Camera megapixel color top-down viewing camera @ 1280 x 1024 pixel	n.a.	25; 12	n.a.	n.a.	n.a.	LED top light, proprietary bi-color multiangle LED lighting
YES Tech	YTV-F1S	position, missing, wrong, polarity, skew	polarity, skew, tombstone, bent lead, lifted, bridging, open solder, insufficient, short, solder balls	Multiple Thin Camera megapixel color top-down and 4 side viewing camera @ 1280 x 1024 pixel	n.a.	25; 12	n.a.	n.a.	n.a.	LED top light, proprietary bi-color multiangle LED lighting
YES Tech	YTV-M1	position, missing, wrong, polarity, skew	polarity, skew, tombstone, bent lead, lifted, bridging, open solder, insufficient, short, solder balls	YESTech 3 Megapixel Thin Camera top-down viewing camera and telecentric lens @ 2048 x 1536 pixel	n.a.	25; 12	n.a.	n.a.	n.a.	proprietary Fusion Lighting

Table 9.

http://dx.doi.org/10.5772/51699

Manufacturer	Model	Inspection capacity typical	Board size max. [mm x mm]	Board size min. [mm x mm]	Board warp [mm]	Board clearance top [mm]	Board clearance bottom [mm]	Board thickness [mm]	Board weight max. [kg]	Dual lane capable	Conveyor height [mm]
Agilent Technologies	Medalist SJ50 Series 3	41 sq. cm/sec @ pre-reflow; 32 sq. cm/sec @ post reflow	510 x 510	50 x 50	n.a.	n.a.	n.a.	0.5 - 4.0	3	Yes	n.a.
Agilent Technologies	Medalist SJ50 Series 3 XL	41 sq. cm/sec @ pre-reflow; 32 sq. cm/sec @ post reflow	620 x 620	75 x 50	n.a.	n.a.	n.a.	1.5 - 15	13	n.a.	n.a.
Agilent Technologies	Medalist sj5000	41 sq. cm/sec @ pre-reflow; 32 sq. cm/sec @ post reflow	510 x 510	50 x 50	n.a.	n.a.	n.a.	0.5 - 4.0	3	Yes	n.a.
Amistar Automation Inc.	K2	0.25 sec/screen	330 x 250	50 x 50	+ 0.5; - 1.0	28	25	0.5 - 2.0	n.a.	n.a.	n.a.
Amistar Automation Inc.	K2L	0.25 sec/screen	485 x 410	50 x 50	+ 0.5; - 1.0	28	25	0.5 - 2.0	n.a.	n.a.	n.a.
CyberOptics	Flex HR 8	50 sq. cm/sec	203 x 508	110 x 63	± 0.7	32	3	n.a.	n.a.	n.a.	813 - 965
CyberOptics	Flex HR 12	50 sq. cm/sec	305 x 508	110 x 63	± 0.7	32	3	n.a.	n.a.	n.a.	813 - 965
CyberOptics	Flex HR 11	50 sq. cm/sec	457 x 508	110 x 63	± 0.7	32	3	n.a.	n.a.	n.a.	813 - 965
Machine Vision Products	Ultra IV	90 sq. cm/sec	500 x 546	n.a.	n.a.	n.a.	n.a.	n.a.	n.a.	n.a.	n.a.
Mirtec	MV-7	4.94 sq. mm/sec	350 x 250	50 x 50	n.a.	25 - 45	50.8	n.a.	n.a.	n.a.	n.a.
Mirtec	MV-7L	4.94 sq. mm/sec	500 x 400	50 x 50	n.a.	25 - 45	50.8	n.a.	n.a.	n.a.	n.a.
Mirtec	MV-7xi	4.94 sq. mm/sec	510 x 460	50 x 50	n.a.	25 - 45	50.8	n.a.	n.a.	n.a.	n.a.
Mirtec	MV-7U	4.94 sq. mm/sec	660 x 510	50 x 50	n.a.	25 - 45	50.8	n.a.	n.a.	n.a.	n.a.
Omron	VT-RNS-S	0.25 sec/screen @ 10 sq. mm field of view	510 x 460	50 x 50	n.a.	20 - 40	40 - 50	n.a.	n.a.	n.a.	n.a.
Omron	VT-WIN II	0.40 sec/screen	460 x 510	50 x 50	n.a.	50	50	0.3 - 4.0	n.a.	n.a.	n.a.
Saki	BF-Frontier	24 sec/screen	460 x 500	50 x 60	± 0.2	40	40	0.6 - 2.5	n.a.	n.a.	max. 900
Saki	BF-Planet-X	23 sec/screen	250 x 330	50 x 60	n.a.	20	30	0.6 - 2.5	n.a.	n.a.	max. 900
Viscom	S3088-III	20 - 40 sq. cm/sec	508 x 508	n.a.	n.a.	35	40	n.a.	n.a.	n.a.	850 - 960
Viscom	S3088-II	20 - 40 sq. cm/sec	450 x 350	n.a.	n.a.	35	40	n.a.	n.a.	n.a.	850 - 960
Viscom	S6056-ST1	20 - 40 sq. cm/sec	457 x 356	n.a.	n.a.	35	60	n.a.	n.a.	n.a.	830 - 960
Viscom	S6056-DS1W	20 - 40 sq. cm/sec	457 x 356	n.a.	n.a.	35	60	n.a.	n.a.	n.a.	830 - 960
Viscom	S6056-DS2W	40 - 80 sq. cm/sec	457 x 356	n.a.	n.a.	35	60	n.a.	n.a.	n.a.	830 - 960
Vi Technology	3K Series	4 - 20 ms	458 x 406	50 x 50	n.a.	34	34	0.7 - 4.0	3	Yes	n.a.
Vi Technology	5K Series	4 - 20 ms	533 x 533	50 x 50	n.a.	34	60	0.5 - 4.0	3	n.a.	n.a.
Vi Technology	7K Series	4 - 20 ms	533 x 610	50 x 50	n.a.	34	60	0.5 - 4.0	3	Yes	n.a.
Vi Technology	Vi-5000	4 - 20 ms	508 x 458	50 x 50	n.a.	34	40	0.7 - 5.0	7	n.a.	n.a.
Vi Technology	Vi-5000-2	4 - 20 ms	508 x 458	50 x 50	n.a.	34	40	0.7 - 5.0	7	n.a.	n.a.
Vi Technology	Vi-5000-3	4 - 20 ms	508 x 458	50 x 50	n.a.	34	40	0.7 - 5.0	7	n.a.	n.a.
YES Tech	YTV-F1	35 sq. cm/sec	560 x 510	n.a.	n.a.	50	50	n.a.	n.a.	n.a.	n.a.
YES Tech	YTV-F1S	35 sq. cm/sec	560 x 510	n.a.	n.a.	50	50	n.a.	n.a.	n.a.	n.a.
YES Tech	YTV-M1	35 sq. cm/sec	350 x 250	50 x 50	n.a.	25	50	n.a.	n.a.	n.a.	max. 950

Table 10. Comparison of Universal Automatic Optical Inspection (UAOI) machines

Assuming that the component is fully operational, these systems practically are able to prove that the whole circuit board is working correctly thus replacing the ICT. However, because they are usually connected to SPC (Statistical Process Control) servers, they can also provide much information about the SMT process itself and provides help as to how to improve it.

But of course there are disadvantages to using AOI systems. They are not able to inspect hidden failures such as soldered BGA (Ball Grid Array) bumps and usually the parameters of inspection algorithms cannot be adjusted perfectly. So from time to time they do not detect real failures which are called 'slip-through failures'. These are the most significant malfunctions during the operation of AOI systems because in these cases, they fail to do what they were programmed for. So the number of slip-throughs must be zero and - if they arise - close investigation is necessary to prevent and eliminate them. However if this occurs repeatedly,

then the appropriate parts would seem to be defective. These are the pseudo-failures which can reduce productivity so their number should as close to zero as possible. [164] ALSO indicates some other image processing problems. The problems of AOI systems will be described in more detail later in the chapter.

Another disadvantage is that they are usually in the 'bottle-neck' of the manufacturing production line because they are not able to inspect the whole circuit board as fast as the line can produce them. Therefore, the practice is usually to place more machines behind each other to enable inspections to take place in parallel. Of course, this also has financial implications which should be taken into consideration.

7. Special AOI solutions — Inspection of lead-free solder joints, flexible substrates, wire bonding and semiconductors

According to RoHS and WEEE directives, lead-free solder alloys have to be used in commercial electronics. This has presented a new challenge for AOI systems because of the differing optical properties of lead-free alloy. Some solutions are shown in the following studies [166]-[173]. AOI has several further application possibilities in electronic device manufacturing e.g. semiconductor and wire-bonding inspection. These appliances need extremely high-resolution cameras to detect defects in the μm scale. Another interesting area is flexible substrate inspection. Some of these special inspections are described in [174]-[179].

7.1. Differences between lead-based and lead-free solder alloys

Solders that contain lead are available with a tin content of between 5% and 70%. The composition of the most commonly used lead solder is 63/37 Sn/Pb; this was the main type used in electronics manufacturing until strict controls were imposed on its use for environmental reasons. The homogeneity of the solder meniscus that formed was beneficial in that the melting point of eutectic solder really is manifested as a single point on the phase diagram; in other words the molten alloy solidifies at a specific temperature, rather than within a broader temperature range. The solidified alloy can be broken down into tiny lead and tin phases of almost 100% purity, without intermetallic layers.

In the case of non-eutectic solders, the crystallisation begins around cores of differing composition and crystal structure, and at differing temperatures, so that during the accretion of the individual cores the composition of the residual melt also changes. Due to this, in the case of lead-free, non-eutectic solder alloys, certain phases solidify earlier, and these solid cores do not form a completely mirror-like, smooth surface on the face of the solder meniscus (and naturally, they also cause differences in the volume of the material).

Lead-free solders usually contain tin, silver and copper. Compared to lead-based solders they have several negative properties: they are more expensive, their melting point is higher, and they give rise to problems that do not occur when soldering with lead (the phenomenon of whisker formation has still not been fully explored). Because their surface differs from that of

http://dx.doi.org/10.5772/51699

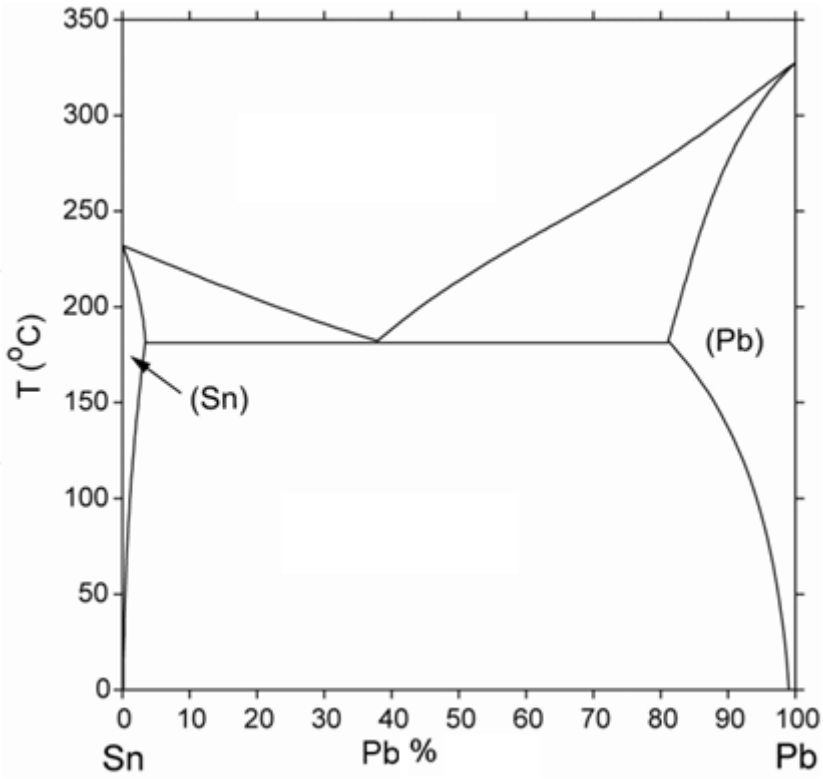

Figure 7. Tin-lead phase diagram

lead-based solder alloys – which are much more even and mirror-like – they reflect light differently, so different procedures may be used to verify the presence and quality of the solder menisci.

In the case of tin-lead solders, the solidification of the melt begins around the cores that are solid at melting point, and the individual solid phases grow at a virtually consistent rate as the two elements separate from the melt. This is how the volumes that are rich in lead and tin become a smooth-surfaced alloy consisting of lead and tin patches, typical of eutectic solder, that can easily differentiated on the cross-section.

Lead-free solders do not usually form eutectic alloys, and exist in many variants with different compositions. Tin is usually alloyed with copper and silver, but there are also alloys containing, for example, bismuth and indium.

In the case of the non-eutectic alloys (the vast majority of lead-free alloys), however, one of the phases begins to solidify earlier, and the alloying metal concentration of this phase will be smaller than that of the melt. This means that the composition of the remaining part of the alloy, which is still in a liquid state, continues to change until the eutectic composition is

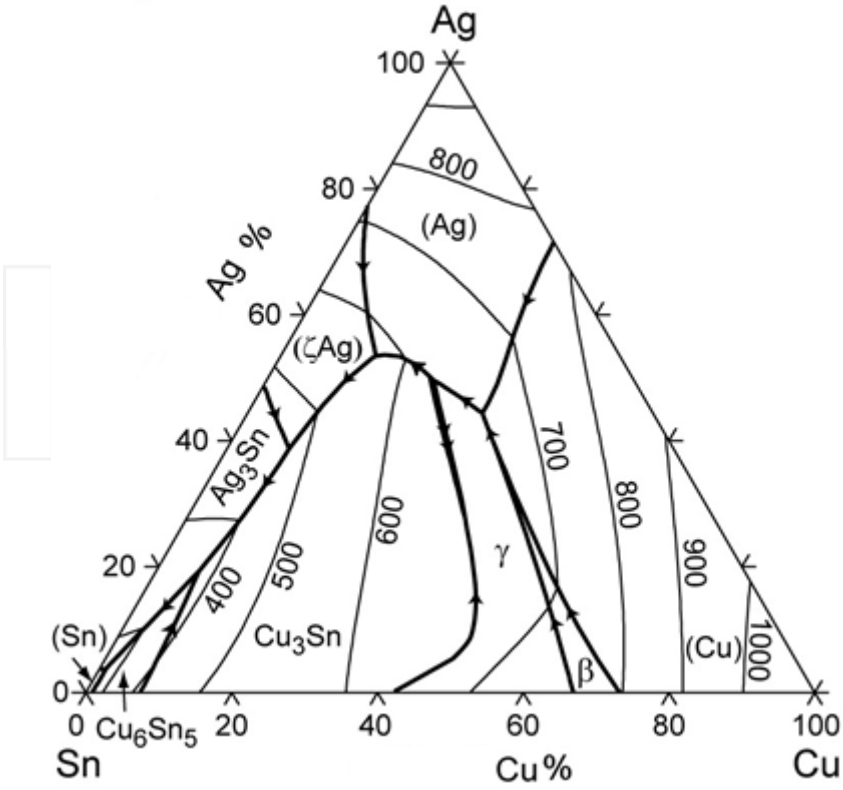

Figure 8. Tin-copper-silver phase diagram

achieved, when it cools and solidifies. As a result of this, the microstructure that is created has a greater surface roughness than in the previous case: as the eutectic melt ebbs away, the intermetallic crystals that were the first to solidify create a more irregular surface. This surface scatters light much more than the smoother, more even surface of the tin-lead solder; in other words the proportion of diffuse reflection will be greater than that of specular reflection.

An attempt to measure the two solders with AOI equipment using the same settings will probably result in several errors, because after the necessary image conversion procedures the images made by the equipment will differ. For this reason, it would clearly be useful to calibrate the AOI equipment specifically for the different solders.

In what follows we present a series of images of tin-lead eutectic and lead-free Sn-Ag-Cu solder alloys made using a scanning electron microscope (SEM). This instrument is not suitable for measuring the surface roughness, but it does provide an accurate, high-resolution image of the examined surfaces and of the two solder alloys with differing composition and surface roughness, showing the differences in height and material with spectacular contrast.

http://dx.doi.org/10.5772/51699

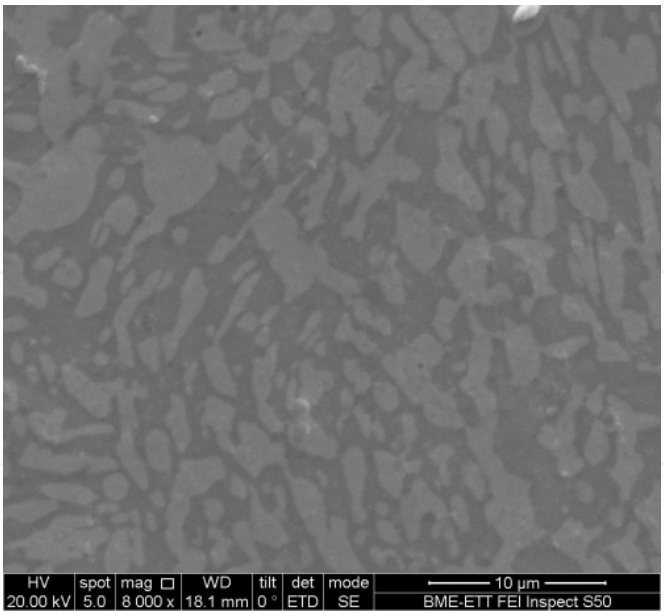

Figure 9. Electron microscope image of the surface of a tin-lead solder meniscus

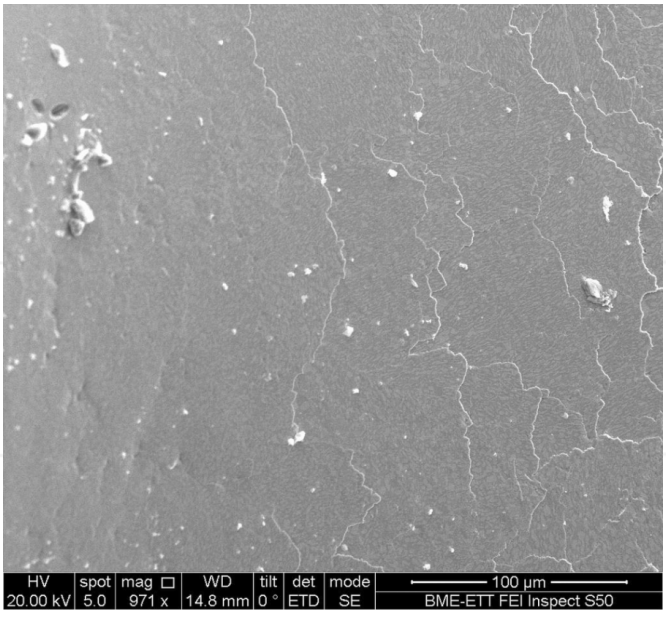

Figure 10. SEM image of the surface of a lead-based solder meniscus

An important question is precisely what the roughness of the pattern formed on the surface of lead-free solder alloys depends on, and how "reliably" predictable the process of its formation is.

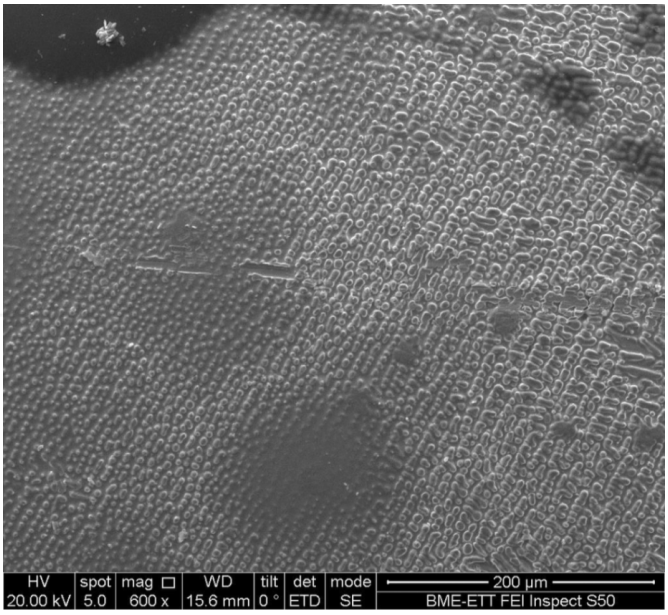

Figure 11. SEM image of the surface of a lead-free solder meniscus

In the above image the two types of solder can be clearly differentiated due to the rougher surface that is typical of the lead-free alloy. In places the surface looks quite similar to the one assumed by the microfacet model, which simplifies reality for the purpose of mathematical manageability; in other words, small semi-spherical formations can be observed side by side with each other. On other parts of the picture, however, areas with no unevenness are also visible; and we have taken the electron microscope image of an area that gives a good illustration of a particular property of lead-free, non-eutectic solder alloys (in this case a tin-copper-silver alloy), namely that due to the unevenness of the surface it reflects the light more diffusely (in other words, it scatters the light more) than the smoother surface of a eutectic solder. In the applied Cook-Torrance model, the roughness of the surface is described by a single parameter, which describes the surface in average terms.

The above picture shows an SEM image of a cross-section in which the tin (light) and lead (dark) phases of the eutectic alloy are clearly differentiated.

The above image was made at a lower magnification (400x rather than 1500x), but the phase boundaries can still be made out, and the smooth meniscus surface typical of lead-based solder

http://dx.doi.org/10.5772/51699

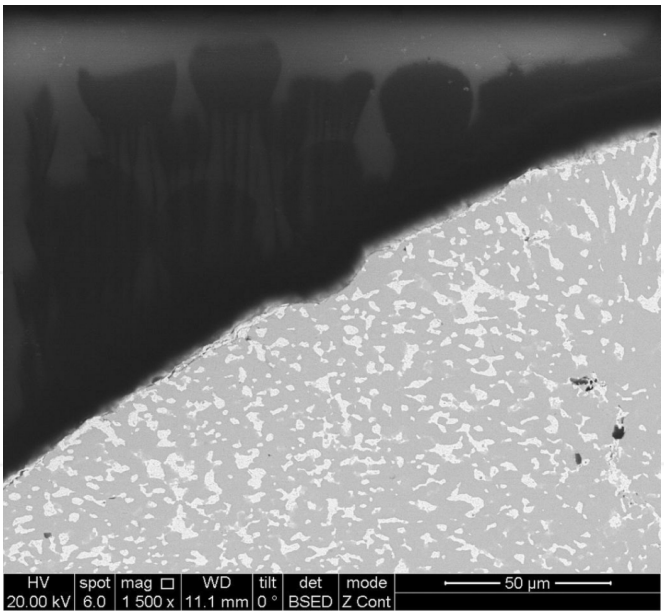

Figure 12. SEM image of a cross-section of a lead-based solder meniscus

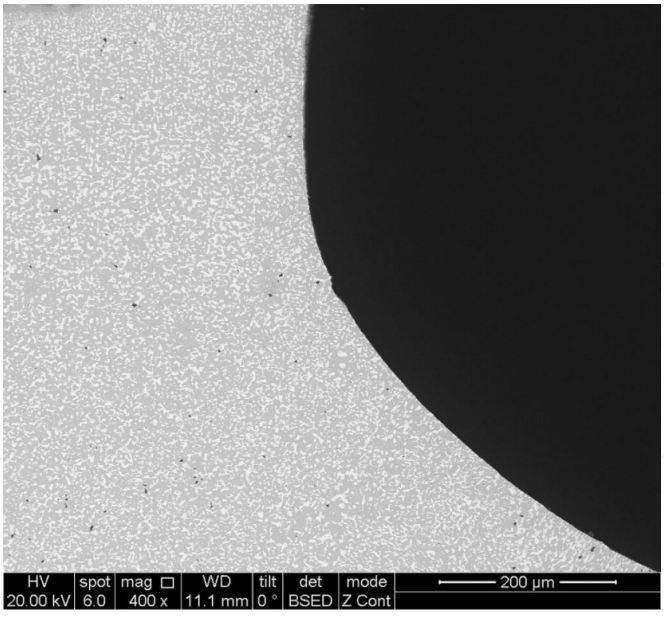

Figure 13. SEM image of a cross-section of a lead-based solder meniscus

alloys is even more visible. In the following SEM images the rough surface typical of lead-free solder alloys can be observed.

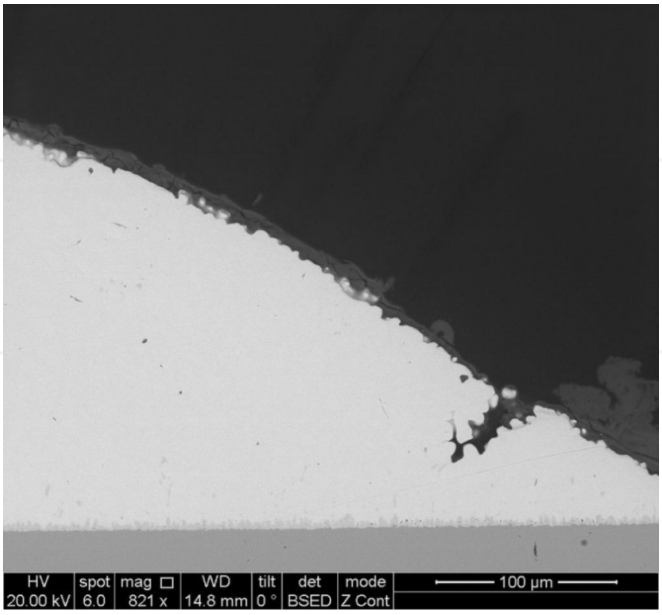

Figure 14. SEM image of a cross-section of a lead-free solder meniscus

The fracture in the solder meniscus seen in the above image is probably due to a contaminant, but within the fracture is a particularly clear example of just how uneven a surface can be formed by the lead-free solder alloy.

The surface roughness of the lead-free solder meniscus is visibly greater than that of the tin-lead solder. Taking the scale bar as a guide we can also estimate that the size of the uneven protrusions that increase the surface roughness, in terms of both their breadth and height, is in the order of 10 μm. It is also worth noting that the simplification of the microfacet model described by the Cook-Torrance model is clearly visible, as a visual inspection reveals that the surface is not closely similar to the surface made up of tiny flat plates that is assumed by the microfacet model. This simplification, however, is more than made up for by the model's simplicity and general ease of use.

7.2. Measuring the surface roughness

To measure the surface roughness we used a Tencor *Alpha Step* 500 surface profilometer. Based on the 10 measurements of each solder, made on the lead-based (Heraeus F816 Sn63-90 B30) and lead-free (Senju Ecosolder M705-GRN360-K1-V) joints, the two solders yielded the following values:

http://dx.doi.org/10.5772/51699

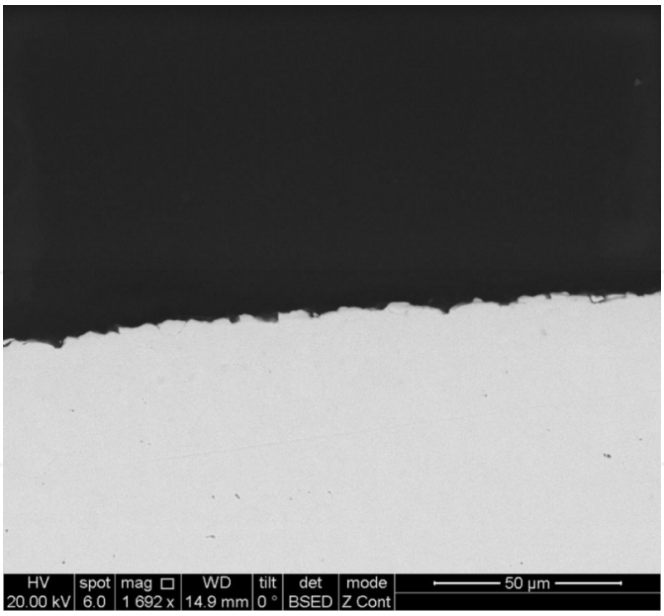

Figure 15. SEM image of a cross-section of a lead-free solder meniscus

Type of measurement result	Lead-based solder paste	Lead-free solder paste
Measured surface roughness (RMS)	0.03092	0.0986
Distribution of measured RMS value	0.004451	0.054626

Table 11. Measured surface roughness values

At first glance the measured surface roughness values appear realistic; the surface roughness of the lead-free solder turned out to be approximately three times that of the lead-based solder. The distribution of the roughness values for the lead-based solder was below 1%, which is satisfactory because the divergence between the shape of the actual solder and that modelled by the computer showed a greater error (a few percent), and because greater fluctuation than this can be expected to result from the differing heat profiles, printed circuit boards or solder-handling requirements of real production lines. The distribution of the surface roughness values for the lead-free solder was over 5%, which is due to diversity of the size and shape of the surface protrusions that appear with this type of solder, which the Cook-Torrance model handles using statistical simplification, by assuming the surface to be of a consistent roughness.

7.3. Simulation created with the computer model

We checked the measured surface roughness values by comparing the images made using optical microscopes with the computer-generated graphic representations. The Surface

Evolver software uses finite element analysis to calculate the surface profile at certain points on the surface. In areas with a greater radius of curvature, where the energies are closer to each other in terms of magnitude (in other words none are dominant in comparison to any others) the software uses more measurement points, that is a denser grid, for displaying the graphic representation.

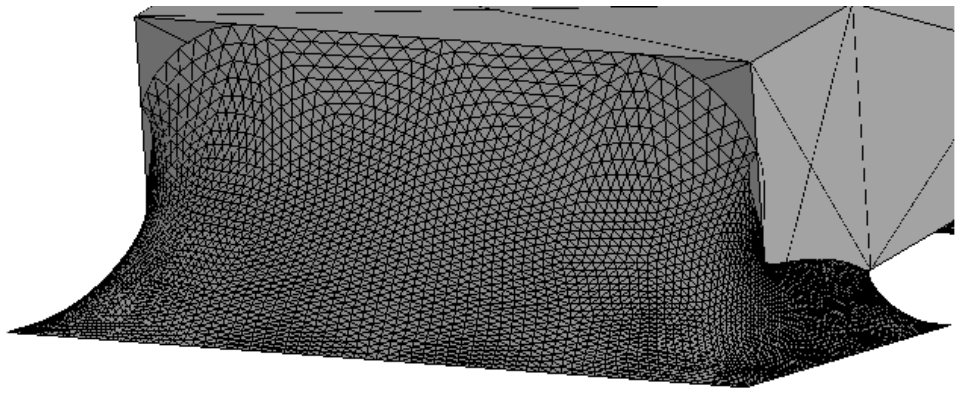

Figure 16. Example of a graphic representation generated using the Surface Evolver software

Of the models that use a formula based on the Bi-directional Reflectance Distribution Function (BRDF), which is based on a physical approach, the most widely used is the Cook-Torrance model, which has surface roughness as one of its input parameters and is also capable of handling Fresnel distribution. During our simulation we used this, in a Direct3D environment, so when generating the rendered graphics we were able to use the measured roughness values as input parameters.

The majority of optical microscopes – including the Olympus BX51 microscope used by me at the department – are capable of operating in bright field (BF) and dark field (DF) imaging mode.

In bright field imaging, both the incident and reflected light fall almost perpendicularly onto the sample, naturally through a focusing lens. Dark field microscopes, on the other hand, collect beams of light that arrive not perpendicularly but from the side, from below a given angle, through a lens, in the direction of the observer; in other words the beams of light travel in the opposite direction but along the same path as would the beams of light that enter perpendicularly but are diffracted, not reflected.

Dark field microscopy gives a good resolution and microscopes with this capability are usually more expensive, but they are eminently suitable for the detection of phase boundaries or the examination of surface irregularities highlighted by the side illumination. In the case of metals, in which the proportion of diffuse components is smaller and the incident light is reflected much more in accordance with the principle of optical reflection, bright field microscopy

http://dx.doi.org/10.5772/51699

results in a darker image and in the case of observation along the z axis (from above), as is typical of microscopes, only the surfaces that are parallel to the horizontal are illuminated. We also modelled both of these different types of illumination using the Direct3D software.

What follows is a comparison of the images made using the optical microscope and the graphic representations rendered with Direct3D that most closely replicated the actual light and surface conditions. Where not indicated separately, the soldered joint (at the SMT resistors) is illuminated with scattered light.

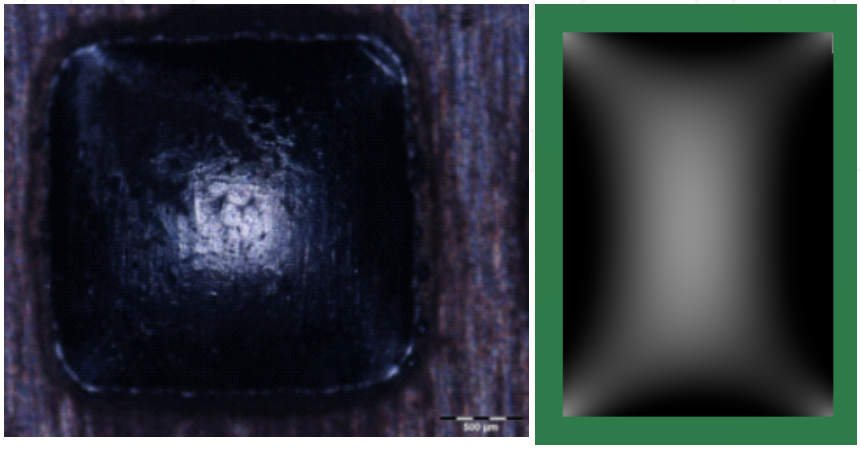

Figure 17. Photograph and graphic representation of empty solder pad covered in lead-free solder (BF imaging)

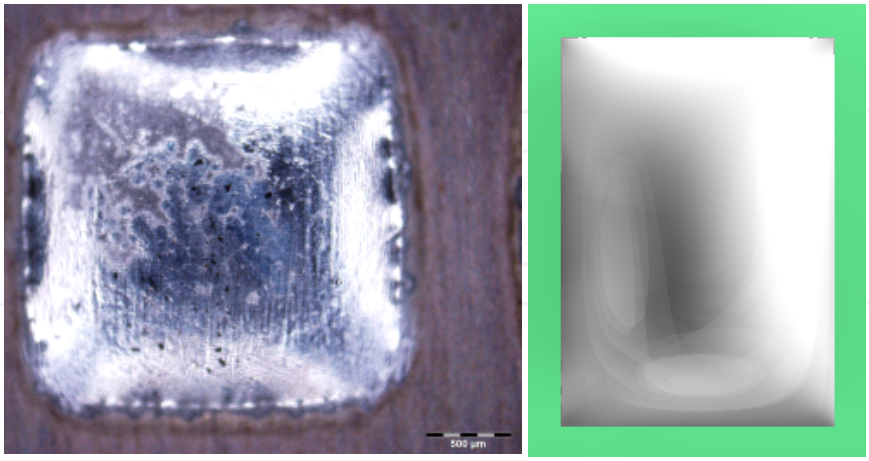

Figure 18. Photograph and graphic representation of empty solder pad covered in lead-free solder (DF imaging)

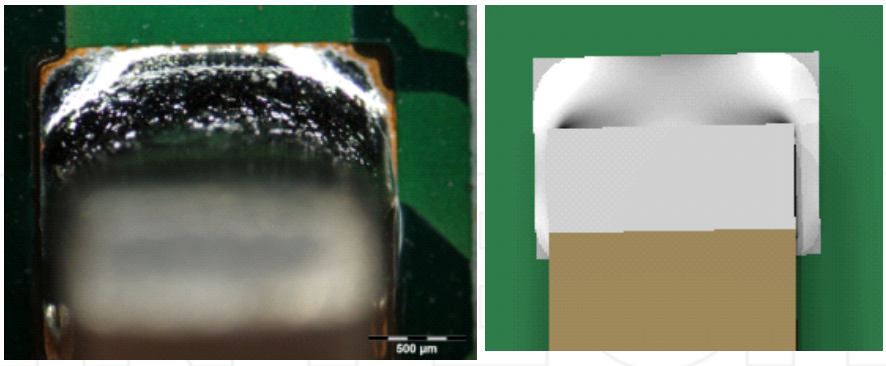

Figure 19. Photograph and graphic representation of SMT joint made with lead-free solder

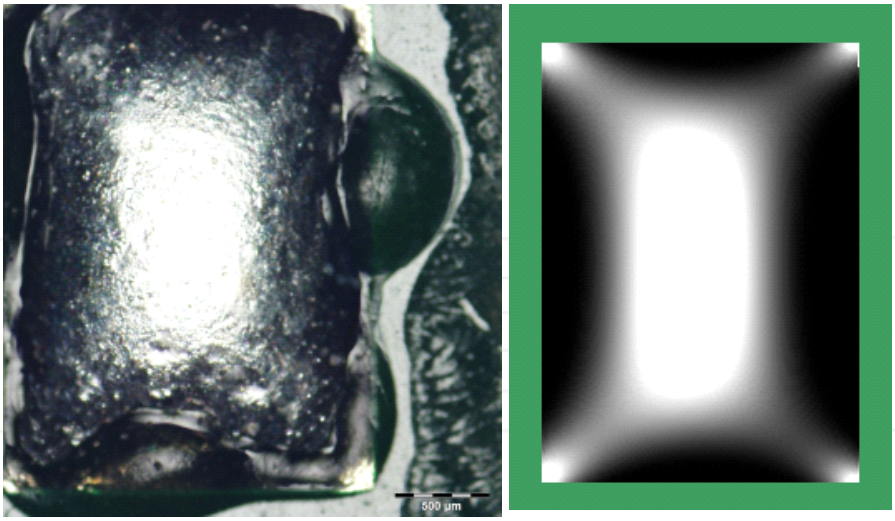

Figure 20. Photograph and graphic representation of empty solder pad covered in lead-based solder (BF imaging)

http://dx.doi.org/10.5772/51699

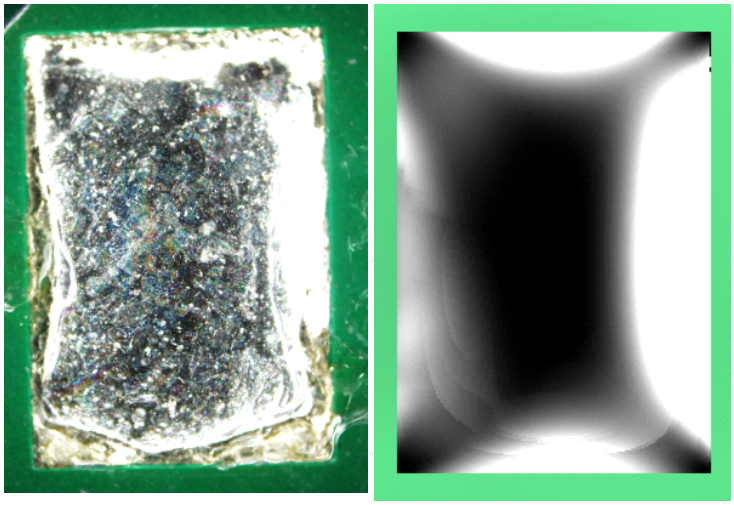

Figure 21. Photograph and graphic representation of empty solder pad covered in lead-based solder (DF imaging)

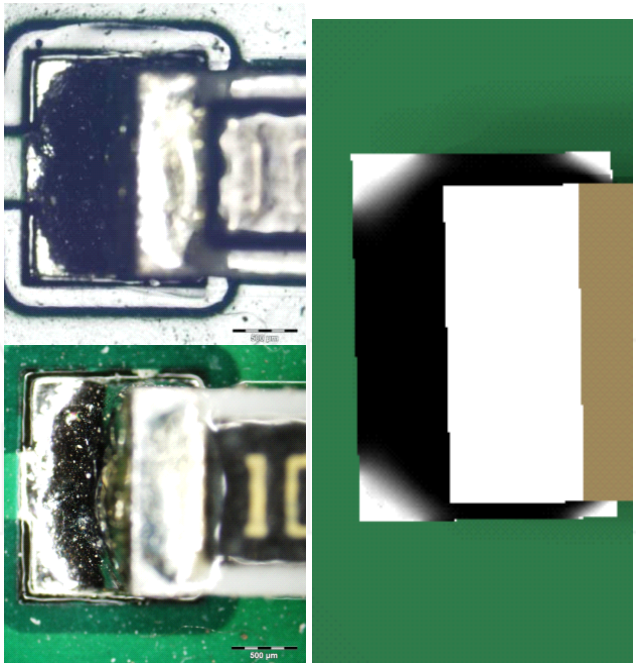

Figure 22. Photographs (above: BF, below: DF) and graphic representation of SMT joint made with lead-based solder

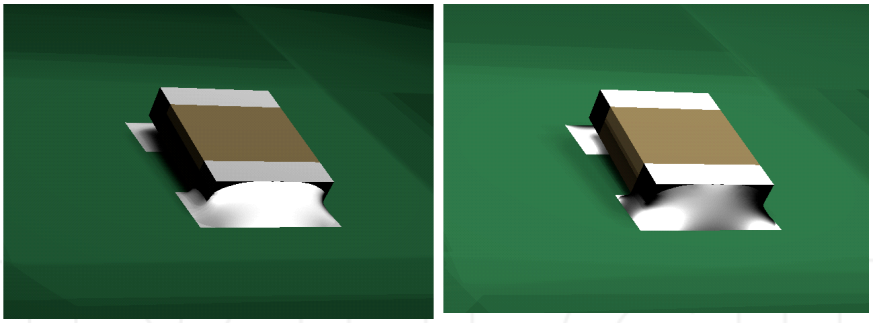

Figure 23. Photograph and graphic representation of SMT joint made with lead-free (left) and lead-based (right) solder

8. Detailed analysis of AOI systems

As can be seen in the previous section, AOI machines handle several tasks. Much literature is dedicated to the intelligence of these systems, but from a technical point of view we can also examine other aspects. A large number of these AOIs work on high-mix-high-volume SMT lines where the most important key factors are the inspection duration and quality. The attributes of this system relate to the following sections:

1. actuating parts (drives and axes)
2. image acquisition system (sensors, optics, illumination)
3. software processing part

They work in close relationship to each other, so the speed of each has to be in sync. There are three well-defined mechanical constructions for an AOI system:

- without special moving parts / drives inside
- with PWB positioning table
- with camera-module actuating unit

The simplest case is when the working-process of the system does not include special positioning steps. The PWB is positioned/placed in "one step" into the field of camera system, an image is acquired and the PWB is then taken out for the next process. This could be of great benefit because the machine does not need to synchronize any movements during the image acquisition process. The speed affecting factor can thus be ignored. This is used typically in Automatic Final Inspection (AFI) systems. This does not mean that the system has to only contain one camera. For more complex applications the number of cameras can be increased. More cameras mean more complex image transformation and manipulation tasks so it follows that these systems are only capable of use when looking at pre-defined areas.

http://dx.doi.org/10.5772/51699

In case of larger inspection areas, the systems are mounted with special drives which can move the camera system or the inspected part. The movements of these drives have to be synchronized with the process of illumination and image acquisition. When the system contains small number of cameras and the illumination devices are also built-in, then the module itself should be the moving section. When there are even more cameras, each with its separate illumination (matrix arrangement), then the PWB should lie on a positioning table.

Two big groups of drive systems are commonly used for this purpose. The first is the conventional electromechanical drive. It is used for some 2D paste inspection machines. Here the velocity of the camera can be constant, while in most cases it contains line-CCD sensor. The other type of motion system is the linear drive which is more accurate and faster and therefore in more frequent use.

The directional route of the moving part highly depends on a second factor, that of speed and the properties of image acquisition system. Here also, three main parts can be singled out:

- optics / lenses
- camera / sensor type
- illumination module / lighting source

The system has to get the necessary amount of information and resolution from even the smallest components. In the SMT field this means zooming down to a 10μm pixel resolution. To ensure the constant magnification at all points of the entire Field of View (FOV) the use of telecentric optics is essential. This criterion enables the system to make the required size-measurements. On an image seen through traditional lenses, the apparent shape of components changes with the distance from the centre of the FOV, therefore sometimes making shape recognition a hard task.

But it is not just the permanency of magnification that is important, so too is the need to select the correct level. On one hand, the larger detection area of the image sensor can help solve this task, but it also increases the computational resources needed. On the other hand, higher magnification levels give a better resolution but at the expense of reducing the field of view. The best scenario is if the system is capable of optional magnification. Generally, a relative large FOV, between 10-25 cm2, could be used and only in certain cases should dedicated Field of Interests (FOI) should be zoomed out.

In most AOI applications, the LED based lighting is used for illumination purposes. But independent of the type of illumination source used, the amount of illumination should be only as much as is required. The optimum depends on the application. For example, a 2D paste or a through-hole-technology (THT) components solder-joint inspection system needs only just a small amount of illumination. As the number of failure types / inspection tasks increase so too the number of illumination modes also increase. The programmable illumination module is a good tool to develop lighting requirements for dedicated purposes, but it also carries the risk of inhomogeneous and reduced FOV.

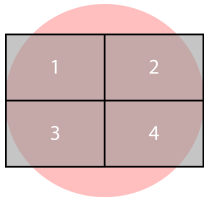

Ring illumination around 4 cameras

23	11	4	-1	-3	-3	0
21	10	3	-2	-5	-5	-2
21	10	3	-1	-2	-2	0
26	15	8	4	2	3	6
34	24	16	13	11	12	15

Grey-level distribution of 1 section

Ring illumination around 1 camera

45	31	21	19	21	34	47
38	22	9	6	9	22	40
36	18	4	2	5	19	37
32	16	2	-3	3	16	33
44	28	16	14	18	44	30

Grey-level distribution of 1 camera

Figure 24. Problem of inhomogeneous grey-level by ring-illumination types

Fig. 7 illustrates two types of camera-illumination systems. The first system contains 4 cameras, the second only 1 camera. Both have LED-ring illumination modules. The grey-level distribution maps shown above have been measured with the same type of illumination and grey-reference flat. The green areas indicate the valuable field of the camera. This example clearly points out the importance of the homogeneity. Of course this phenomenon is also present when the illumination system is multi-coloured.

Most optical inspection / control appliance decisions are based on image-processing methods that have been set experientially. The stress is on the word “experientially”. Most of the AOI machines make some kind of template matching. These sample-templates can be colour or greyscale, stand from parts/windows or form a complete pattern. The machine can be ‘self-learning or directed by means of an “external trainer”. Due to the fact that the overall reliability of these machines is not 100%, the defined limits between good and bad classified patterns are not strict. In some cases it could be that just two pixels differ between the data provided. If the phenomenon which the system needs to detect is not so unambiguous, then it should search for another method to make the gap wider between the 2 classes.

9. Software questions

One of the most wide-spread criticisms against the principles and methods of automated optical inspection systems stems from a very interesting paradox. As we have mentioned earlier, the introduction of AOI devices in the manufacturing lines was a result of the growth in manufacturing process complexity. These inspection and control devices have to fulfill certain reliability criteria which need to be validated. But unfortunately, these validation

http://dx.doi.org/10.5772/51699

processes can only be used to a limited degree because of the high-complex manufacturing process and the equally complex and highly varied appearance of devices under test (DUTs).

This contradiction invokes the conclusion that accuracy and reliability of AOI system depends very much on the competence and working quality of the engineers and operators, the correct management of the setting up and controlling the inspection devices. In reality, this sets out several very serious challenges to experts. The quality inspection algorithms have many parameters – in some cases several hundred – (image processing, region of interest, threshold parameters etc.). Their setup requires experience, intuition and inspiration from the process engineers themselves.

In addition, during parameter tuning, the engineers need to solve the following contradiction, where the difference between images showing correct and faulty components is often only a few pixels which need to be detected by the AOI devices (Fig. 8). In the case of incorrect parameter settings these small signals can disappear and the system classify a bad component as good ("slip-through"). Certainly this false classification is totally intolerable in quality inspection processes; therefore it is necessary to aim for the complete elimination of this possibility by fine tuning the algorithm's parameters. Unfortunately because of this, engineers can easily set the algorithm to be too strict, meaning also that some correct components will be dropped out during the inspection process. Although these "false calls" (also known as pseudo failure) do not cause catastrophic consequences nevertheless they are the source of a very serious problem. Namely, in this instance, the human operators performing the re-inspection of components considered "faulty" can easily get used to the repeated mistakes of the AOI system. Therefore they can eventually take the inspection device's decisions out of consideration even where there is a cases of real errors. This implies that the reliability of the inspection device itself would be in doubt; the fact of which would result in one of the biggest catastrophic effects on AOI systems. In addition, it seems insignificant but it is important to note that many bad classifications slow the manufacturing process, decrease productivity and increase the product overall production costs. To avoid false calls, process-engineers need to reduce the strictness of the inspection parameters which – as we have mentioned earlier – is inconsistent with principle used by the parameter settings preventing the slip-through.

Figure 25. An example for the tiny differences between the images containing correct and faulty components

In addition, AOI engineers need to cope with several other difficulties a major one of which is that the production process changes continuously e.g. the settings of devices on the manufacturing line have to be modified, and this needs to be followed also by modifications to the AOI devices. Therefore the need to monitor the inspection algorithms and adapt to different parameters is a serious challenge to the process engineers.

Furthermore, it is necessary to satisfy some practical requirements when selecting and adjusting the inspection algorithms. Usually, electronic factories manufacture more products in parallel in which several similar or identical components can be located. If all the components were to be inspected with a separate AOI algorithm, the code management, version tracking and fixing etc. would be impossible. Therefore, engineers often use only one inspection method for similar mountings to achieve simpler AOI algorithm version management. Unfortunately, this strategy cannot always be used successfully because of the very heterogeneous appearance of the same components. Fig.9. shows an image sequence of the C0805 capacitor which illustrates the enormous differences between images taken of similar components.

In this varied environment it is very hard to develop an inspection method which results in highly reliable classification of each type of image for the same component. In addition, a parameter setting process that reduces the number of bad classifications in case of one component influences not only the selected manufacturing line but has an effect on the whole factory. Therefore it can happen that whilst a parameter optimization process reduces the number of bad classifications in the first part of the factory, it increases them on other manufacturing lines. This paradox is one of the reasons why the AOI macro optimization process is a very long and "Sisyphean" task of AOI process engineers.

Figure 26. Differences between the appearances of similar components (capacitor C0805)

A very interesting and important question is the optimization of classification thresholds. One of the most important requirements of an inspection system is high-level robustness, but this condition can hardly be guaranteed if the classification decision (namely whether a component gets "faulty" or "good" label) is dependent on only one pixel. Therefore the quality results close to the decision threshold need to be classified in a separate group ("limit error") and it is necessary to apply a different strategy to them. It follows that AOI experts – apart from the fact that they need to solve the optimization paradox mentioned earlier – have to strive to find such an algorithm parameter setting where during the classification, the number of components classified near the decision threshold are as few as possible. Efficiency of AOI appliances

http://dx.doi.org/10.5772/51699

can be significantly improved with the help of macro optimization. In the first task, the pseudo rate was reduced while slip-throughs remains zero (Table VIII, Fig. 10)

Before optimization (30 days testing period)			
Inspected components (solder joints) [pieces]	Detected failures [pieces]		***Pseudo rate [ppm]***
	Real failures [pieces]	Pseudo failures [pieces]	
347 130 (694 260)	4 676		***13 459***
	4	4 672	

After optimization (30 days testing period)			
Inspected components (solder joints) [pieces]	Detected failures [pieces]		***Pseudo rate [ppm]***
	Real failures [pieces]	Pseudo failures [pieces]	
223 006 (446 012)	52		***224***
	2	50	

Table 12. Results of macro optimization

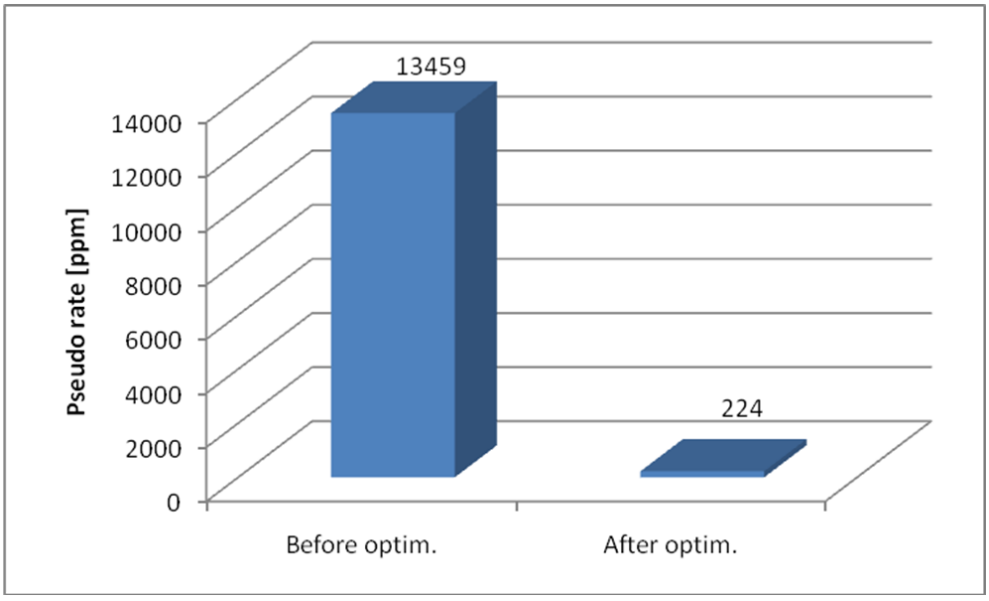

Figure 27. Pseudo reduction

Secondly parallel pseudo and slip-through reduction were carried out (Table IX, Fig. 11, Fig. 12).

Before optimization (30 days testing period)			
Inspected components (solder joints) [pieces]	Detected failures [pieces]		***Pseudo rate [ppm]***
	Real failures (***Quasi-tombstone***) [pieces]	Pseudo failures [pieces]	
2 423 334 (4 846 668)	68 205		***27 995***
	364 (***0***)	67 841	

After optimization (30 days testing period)			
Inspected components (solder joints) [pieces]	Detected failures [pieces]		***Pseudo rate [ppm]***
	Real failures (***Quasi-tombstone***) [pieces]	Pseudo failures [pieces]	
4 655 392 (9 310 784)	58 654		***12 560***
	627 (***62***)	58 027	

Table 13. Results of macro optimization

Another very serious question is about the parameter optimization process, namely how can the AOI engineers validate the new parameter values determined by the optimization process? Certainly a correction of a bad classification cannot be validated only by examination of the specified image, but it is necessary to check several other instances. Therefore, to execute a reliable validation process, the engineers have to collect a large image database ("image base") covering all cases as they occur in the best possible way. Unfortunately, creating a good and usable image base is a long and sometimes impossible task because of several – often contradicting – criteria. A manual image collection by the engineers is very time-consuming and in case of automatic systems (like AOIs) there is only a limited possibility because of the high number and varied type of data. Automatic methods are faster but during the collection, some falsely classified images can be put in the image base which makes the parameter optimization impossible. For example, if an image containing a faulty component is placed into the "good" part of the image base, the optimization process will try to adjust to the parameters that the AOI algorithm has classified the image as "good". As a result, the optimized macro cannot recognize this specified error which can indicate slippages causing the greatest type of inspection catastrophe.

The number of stored images is also a very important factor. If the image base contains too many images, the resources (processor, hard drive, network etc.) become overloaded and the optimization process can only be executed slowly. On the other hand in case of a small image base the algorithm validation is neither reliable nor accurate enough.

http://dx.doi.org/10.5772/51699

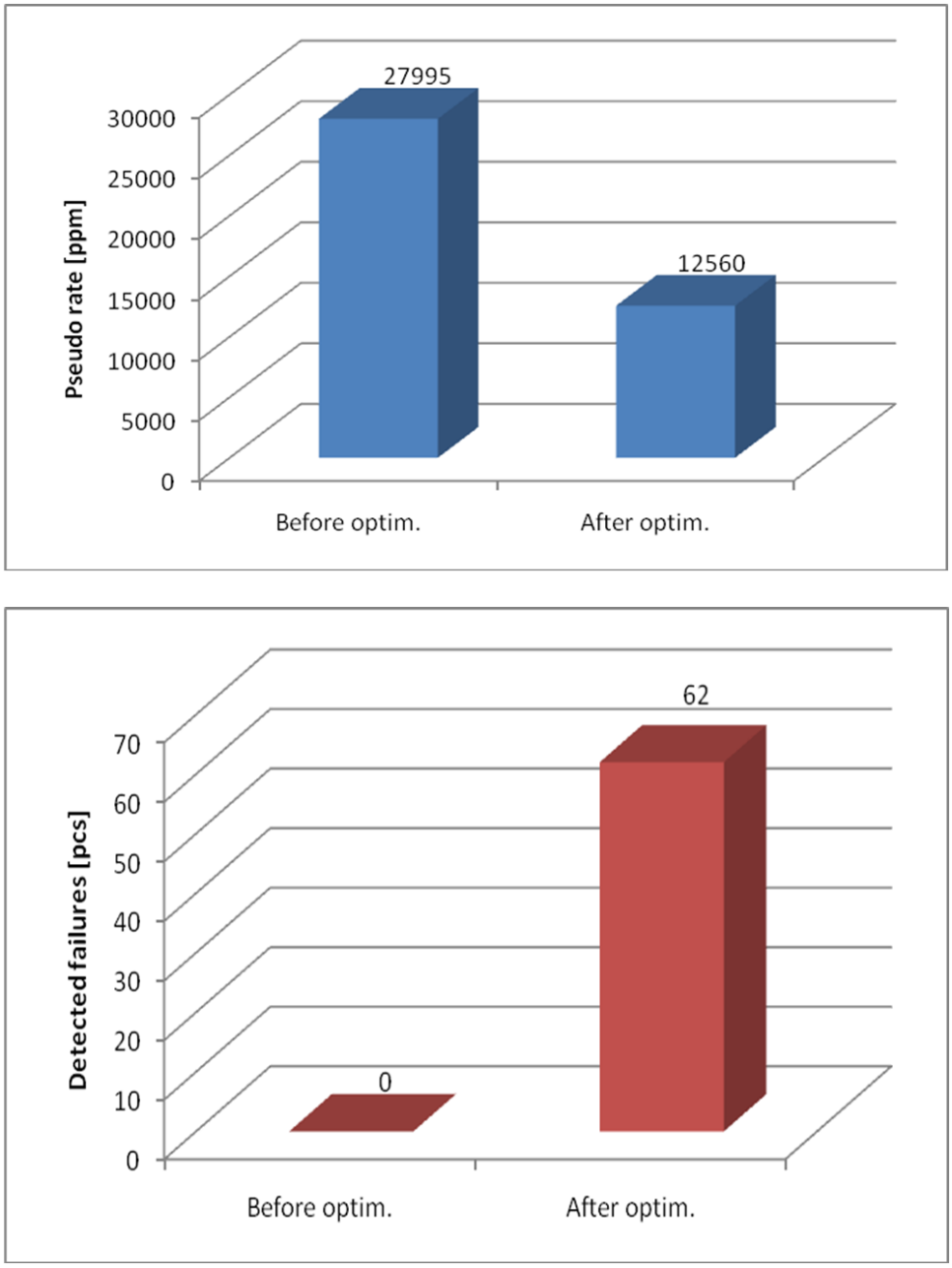

Figure 28. Pseudo and slip-through reduction

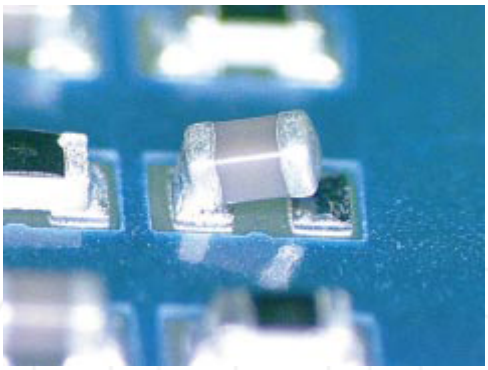

Figure 29. Quasi-tombstone

If we suppose that the optimal size of image base is determined (and which cannot be exceeded) and relevant images are collected resulting in a reasonably good image base. At this point another question arises: how can the engineers update the database with new images? It is very hard to determine which images from the new image-set need to be stored and which images need to be deleted from the current image base. There are several criteria – such as the date created, the number of similar images etc. – which can be used as the basis of the updating decision but a precise numerical factor which shows the usefulness of pictures in the database is much more difficult to determine.

The aspects and concepts mentioned in this section have shown that the usage and perfect operation of automated optical inspection system requires human control and supervision. Although the devices' algorithms are able to execute fast, accurate, efficient, reliable, "assiduous" and continuous inspection (they appear to be much more suitable than human operators as a consequence!) without being fed sufficient intelligence they cannot adapt immediately and independently to changes in manufacturing. Therefore the quality inspection process can hinder the increased spreading of autonomous electronic manufacture.

Several researches and developments are focusing on the problem to redeem the status of the human operators' work and to provide help for AOI engineers. Very interesting research directions are in automatic algorithm parameter optimization methods. The AOI devices on the manufacturing line monitor the quality of the algorithms (number of false calls and slip-through, if possible) and on occasions they adjust the parameters using the image base to create a better, higher quality algorithm. The engineers only need to take care of special cases like changing the lighting or creating new inspection methods. Although the automatic parameter optimization methods do not have to satisfy high real-time criteria, it is important to determine the optimized parameter values in a relatively short time. It is easy to verify that even in the case of having some dozen parameters; the analysis of all parameter-combinations takes a very long time (years) therefore heuristic search methods have to be used to solve the optimization problem.

http://dx.doi.org/10.5772/51699

Certainly the automatic optimization methods also need to collect the relevant images autonomously to create the reference image base. This work sets serious challenges for optimization processes because of the problems and difficulties mentioned earlier.

As a summary, we can establish that AOI systems offer a powerful solution for a complex problem by means of simple principles, but the analysis of details can reveal several problems, difficulties and contradictions. Finding a solution for them is an essential condition for the automated optical inspection systems in the future.

10. 3D Inspection

But the analyze-development is just one route for improving the AOI process. The other is the "extended" optical inspection system with measuring capability. The pioneers of this property are 3D SPI machines. In the last few years, a wide variety of these machines have been developed. The inspection in this application - checking the SMT printing process - means the 3 dimensional measurements of solder paste bumps. These bumps are shaped like cylinders or cubes so that the geometries and surfaces are relative simple. This fact makes the 3D optical techniques a viable option. Several measurement techniques are used for this process, some of these are shown in Fig. 13.

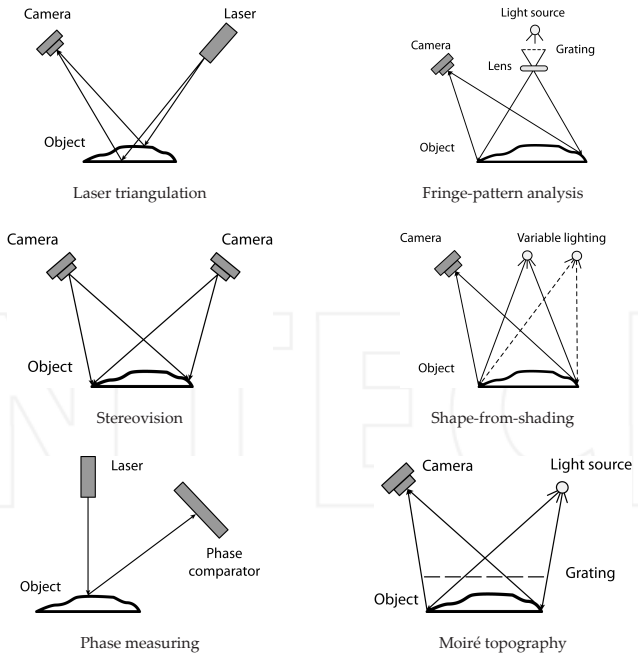

Figure 30. optical measurement techniques

The same is true for inspecting component presence, but for solder-joint detection these technologies are in their infancy at present. The shape of different components' solder-joints is complex and the specular surface also makes the task even more difficult. There have been a number of research efforts, optical 3D shape measurement technologies, based on several technologies as shown in Fig.2. Some of these researches can be found in the following studies [181-198]. Also some companies are in the development phase such as Koh-Young Technology [180]. So the evaluation of these geometries is as yet more difficult, but with the development of optical metrology there will be more AOI machines with measuring capability.

11. Further developments, the future of AOI

AOI systems are following the worldwide trends i.e. multi-task integration, adaptivity, speed, etc. There are already appliances that integrate optical inspection with repair functions: Ersa's AOI+R solution or optical and X-ray inspection together. Some suppliers have AOI+AXI or Viscom's AOXI (simultaneous inspection). Another possible area of development is the inspection speed. Faster image capturing (with larger FOV, faster camera positioning etc), parallel inspection of two PWBs are some possible ways for this to be done.

The other important area is adaptivity. Mainly adaptive illumination is the future of AOI systems. It would help to drastically reduce pseudo-failures rates and eliminate slip-through failures.

A third area is image processing. 3D inspection, neural networks, fuzzy systems, intelligent algorithms which will help to increase the efficiency and reliability of these systems.

12. Conclusion

Inspection systems are widely used to determine the quality of electronics modules after assembly sequences. Nowadays this is usually the automatic, non-contact and non-destructive process, such as automatic optical inspection (AOI), supplemented with automatic X-ray inspection (AXI) if necessary. These appliances inspect the ready or the incomplete printed wiring boards to determine the quality of it's given property in any technological sequence, such as paste printing, component placement or soldering. The rapid development of electronics module assembly manufacturing requiring parallel development of test procedures. The automatic optical inspection is potential multi-disciplinary research area, because from image acquiring, (illumination, the detection of the reflected light etc.) through image processing, to the evaluation each area can be optimized to reach to goal, that the qualification of the inspected object in the field of interest (FOI) by the used appliance, matches the specifications as stated. Most manufacturers agree that, from a strategic point of view, the optical inspection after soldering should not be ignored. As a consequence, this is the most important part of an AOI inspection. The quality of solder joints is determined from geometric and optical properties of the solder meniscus. These parameters determine the reflection properties of the

meniscus. The meniscus forms from the liquid alloy during the soldering process. After cooling, the meniscus becomes solid and reflects illumination which means that we can classify them. From these reflection patterns and with the help of image processing algorithms we are able to determine the quality of the solder joints. As described above, the correct source of illumination is essential. There are several different kinds of approach: white or RGB; directed or diffuse; ring or hemisphere.

This survey gives state of the art review of current automated optical inspection systems in the electronic device manufacturing industry. The aim of the chapter is to give an overview about the development phases, operating mechanisms, advantages and disadvantages of AOI appliances, their technical parameters, field of usage, capabilities and possible trends for further developments.

Author details

Mihály Janóczki[1*], Ákos Becker[2], László Jakab[3], Richárd Gróf[4] and Tibor Takács[5]

*Address all correspondence to: mihaly.janoczki@eu.agc.com

1 AGC Glass Hungary Ltd., H-2851 Környe, Hungary

2 DENSION Audio Systems Ltd., Budapest, Hungary

3 Department of Electronics Technology, Budapest University of Technology and Economics, Budapest, Hungary

4 Epcos AG, Heidenheim, Deutschland

5 Department of Control Engineering and Information Technology, Budapest University of Technology and Economics, Budapest, Hungary

References

[1] Matthew T. Holzmann, Automatic Optical Inspection Of Circuit Assemblies In a High Mix/Low Volume Environment, Christopher Associates, Inc. Santa Ana, California USA

[2] Miran Burmen, Franjo Pernuš and Boštjan Likar, LED Light Sources: A Survey of Quality-Affecting Factors and Methods for Their Assessment, Measurement and Science Technology Vol. 19, No.12, 2008, 122002 (15pp)

[3] Sheng-Lin Lu, Xian-Min Zhang, Yong-Cong Kuang, Optimized Design of an AOI Illuminator, Proceedings of the 2007 International Conference on Wavelet Analysis and Pattern Recognition, Beijing, China, 2-4 Nov. 2007, pp. 924-928

[4] Yuji Takagi, Seiji Hata, Susumu Hibi, Visual Inspection Machine for Solder Joints Using Tiered Illumination, SPIE Machine Vision Systems Integration in Industry, Vol. 1386, 1990, pp. 21-29

[5] Y.J. Roh, D.Y. Lee, M.Y.Kim, H.S. Cho, A Visual Inspection System with Flexible Illumination and Auto-focusing, Proceedings of SPIE, Vol. 4902, 2002, pp. 463-475

[6] Alexander Hornberg, Handbook of Machine Vision, Wiley-VCH Verlag GmbH Co KGaA, Weinheim, 2006

[7] E.R.Davies, Machine Vision: Theory, Algorithms, Practicalities, Elsevier, 2005

[8] Kjell J. Gasvik, Optical Metrology 3rd Edition, John Wiley & Sons Ltd., ISBN: 0-470-84300-4, 2002

[9] Shree K. Nayar, Arthur C. Sanderson, Lee E. Weiss, David A. Simon, Specular Surface Inspection Using Structured Highlight and Gaussian Images, IEEE Transaction on Robotics and Automation, Vol. 6, No. 2, April 1990

[10] Peter Conlon, AOI A Strategy for Closing the Loop, Surface Mount Technology, April 2006, pp. 24-29

[11] Pamela R. Lipson, Imagen and Landrex Technologies, AOI Systems Simulate Human Brain, Test & Measurement World, February 2007, pp. 35-42

[12] Herbert Tietze, Jens Kokott (GOEPEL electronic GmbH), Application of AOI Systems in Backplane Manufacturing

[13] Titus T. Suck (Orbotech), Controlling the Process: Post-Reflow AOI (Automated Optical Inspection) to Ascertain Machine and Process Capability

[14] Don Miller (YesTech), Exploring AOI and X-ray http://www.dataweek.co.za/news.aspx?pklNewsId=31727&pklCategoryID=49, (accessed 12 July 2009)

[15] Mark J. Norris, Advances in Automatic Optical Inspection, Gray Scale Correlation vs. Vectoral Imaging, Journal of Surface Mount Technology, Vol. 15, January 2002

[16] Christopher C. Yang, Michael M. Marefat, Frank W. Ciarallo, Error Analysis and Planning Accuracy for Dimensional Measurement in Active Vision Inspection, IEEE Transactions on Robotics and Automation, Vol. 14, No. 3, June 1998

[17] Jens Kokott, The capability of modern AOI systems, Global SMT & Packaging, November/December 2006, pp. 16-17

[18] Matthew Holzmann, AOI in a High-Mix/Low-Volume Environment, Circuits Assembly, June 2004, pp. 30-35

[19] Keith Fairchild, Evaluating ROI of AXI vs. AOI, Circuits Assembly, October 2006, pp. 20-25

[20] "Realising Expectations of AOI http://www.dataweek.co.za/news.aspx?pklNewsId=30534&pklCategoryID=4914, (accessed 03 July 2009)

[21] David Doyle, Challenges for Second Generation Automated Optical Inspection (AOI) Solutions

[22] K C Fan, C Hsu, Strategic Planning of Developing Automatic Optical Inspection (AOI) Technologies in Taiwan, 7th International Symposium on Measurement Technology and Intelligent Instruments, Journal of Physics, Conference Series 13, 2005, pp. 394-397

[23] Peter Krippner, T&M, Zero-defect IC Inspection Strategy With AOI, 2006 Electronics Manufacturing, March 2006, http://www.emasiamag.com/currentIssue.asp?d=1&m=3&y=2006# (accessed 12 July 2009)

[24] Mukul Shirvaikar, Trends in Automated Visual Inspection, Real-Time Image Processing, Springer, 2006, 1:41–43

[25] Bob Ries, New Advances in AOI Technologies, Surface Mount Technology, January 2001, pp. 62-66

[26] Duncan Nicol, The Key (or Start Button) to Success, EPP Europe, November 2008, pp. 47-49

[27] Douglas W. Raymond, Dominic F. Haigh, Why Automated Optical Inspection, International Test Conference, 1997, pp. 1033

[28] Pamela Lipson, To Be or Not to Be in Color:A 10 Year Study of the Benefits and Pitfalls of Including Color Information in AOI Systems, Proceedings of the IPC APEX Technical Conference EXPO, 2009

[29] Pamela Lipson, Lyle Sherwood, The landscape of PCB Technology is Changing Rapidly. How Will AOI Testing Keep Up?, Proceedings of the IPC APEX Technical Conference EXPO, 2009

[30] Teledyne,DALSA,http://www.teledynedalsa.com/public/dc/documents/Image_Sensor_Architecture_Whitepaper_Digital_Cinema_00218-00_03-70.pdf (accessed 12 July 2009)

[31] Teledyne DALSA Applications Set Imager Choices, Dalsa Aplication Note, http://www.dalsa.com/public/corp/applications_set_imager_choices.pdf (accessed 12 July 2009)

[32] Dave Litwiller, CMOS vs. CCD: Maturing Techologies, Maturing Markets, Reprint from the 2005 August issue of Photonics Spectra, Laurin Publishing

[33] Stuart A. Taylor, CCD and CMOS Imaging Array Technologies: Technology Review, Technical Report EPC-1998-106, Xerox Research Centre Europe http://www.research.microsoft.com/pubs/80353/CCD.pdf (accessed 12 July 2009)

[34] Sharma, A Look at CCD Sensors…, What Digital Camera Magazine; November 1997, pp. 54-56

[35] News Item, CMOS to Signal end of Line for CCD?, What Digital Camera Magazine; June 1997

[36] Dunn, James F.; "A New Digital Camera Startup Busts Price/Performance Standards with CMOS Sensor, Advanced Imaging; January 1997

[37] Young Y. Cha, J.H. Oh, A Field-of-View Generation Algorithm Using Neural Network, Mechatronics Vol. 11, 2001, pp. 731-744

[38] http://en.wikipedia.org/wiki/Barcode#Matrix_.282D.29_barcodes (accessed 12 July 2009)

[39] Ja H. Koo, Suk I. Yoo, A Structural Matching for Two-Dimensional Visual Pattern Inspection, IEEE International Conference on Systems, Man and Cybernetics, Vol. 5, 1998, pp. 4429-4434

[40] Wen-Yen Wu, Mao-Jim J. Wang, Chih-Ming Liu, Automated Inspection of Printed Circuit Boards Through machine Vision, Computers in Industry, Vol. 28, 1996, pp. 103-111

[41] H. Rau, C.-H.Wu, Automatic Optical Inspection for Detecting Defects on Printed Circuit Board Inner Layers, The International Journal of Advanced Manufacturing Technology, Vol. 25, 2005, pp. 940-946

[42] Zuwairie Ibrahim, Zulfakar Aspar, Syed Abdul Rahman Al-Attas, Musa Mohd Mokji, Corse Resolution Defect Localization Algorithm for an Automated Visual Printed Circuit Board Inspection, 28th Annual Conference of the IECON 02, Vol. 4, 2002, pp. 2629-2634

[43] Fikret Ercal, Filiz Bunyak, Hao Feng, Context-Sensitive Filtering in RLE for PCB Inspection, Conference of Intelligent Systems in Design and Manufacturing, Vol. 3517, 1998, pp. 286-293

[44] M Moganti, F Ercal, CH Dagli, S Tsunekawa, Automatic PCB Inspection Algorithms: A Survey, Computer Vision and Image Understanding, Vol. 63, No. 2, March 1996, pp. 287-313

[45] Péter Szolgay, Katalin Tömördi, Optical Detection of Breaks and Short Circuits on the Layouts of Printed Circuit Boards Using CNN, Cellular Neural Networks and their Applications, Fourth IEEE International Workshop, 24-26 Jun. 1996, pp 87-92, DOI: 10.1109/CNNA.1996.566498

[46] Ji-joong Hong, Kyung-ja Park, Kyung-gu Kim, Parallel Processing Machine Vision System for Bare PCB Inspection, IEEE, 1998, pp. 1346-1350

[47] Madhav Moganti, Fikret Ercal, Cihan H. Dagli, Shou Tsunekawa, Automatic PCB Inspection Algorithms: A Survey, Computer Vision and Image Understanding, Vol. 63, No. 2, March, 1996, pp. 287-313

[48] Timót Hidvégi, Péter Szolgay, Some New Analogic CNN Algorithms for PCB Quality Control, International Journal of Circuit Theory and Applications Archive, Vol. 30, Issue 2-3, March 2002, pp. 231-245

[49] Fabiana R. Leta, Flávio F. Feliciano, Flavius P. R. Martins, Computer Vision System for Printed Circuit Board Inspection, ABCM Symposium Series in Mechatronics, Vol. 3, 2008, pp.623-632

[50] Noor Khafifah Khalid, Zuwairie Ibrahim, and Mohamad Sshukri Zainal Abidin, An Algorithm To Group Defects On Printed Circuit Board For Automated Visual Inspection, IJSSST, Vol. 9, No. 2, May 2008, pp. 1-10

[51] Nam Hyeong Kim, Jae Young Pyun, Kang Sun Choi, Byeong Doo, Choi, SungJea Ko, Real-Time Inspection System for Printed Circuit Boards, Lecture Notes in Computer Science, Vol. 2781, 2003, pp. 458-465

[52] Amistar Automation Inc.: K5/K5L Desktop Board Inspector, Data Sheet, Updated November, 2007

[53] Lloyd Doyle Limited duotech, Data Sheet, Updated Septembe, 2005

[54] Lloyd Doyle Limited Excalibur 5000 X2, Data Sheet, Updated September, 2005

[55] Lloyd Doyle Limited LD 6000, Data Sheet

[56] Lloyd Doyle Limited phasor, Data Sheet, Updated September, 2005

[57] Lloyd Doyle Limited redline, Data Sheet, Updated September, 2005

[58] I. Fidan, R. P. Kraft, L. E. Ruff, S. J. Derby, Designed Experiments to Investigate the Solder Joint Quality Output of a Prototype Automated Surface Mount Replacement System, IEEE Transactions on Components, Packaging, Manufacturing Technology, Vol. 21, No. 3, Jul. 1998, pp. 172-181

[59] J. Pan, G. L. Tonkay, R. H. Storer, R. M. Sallade, D. J. Leandri, Critical Variables of Solder Paste Stencil Printing for Micro-BGA and Fine Pitch QFP, Proceedings on the 24th IEEE/CPMT International Electronics Manufacturing Technology Symposium, 1999, pp. 94-101

[60] D. He, N. N. Ekere, M. A. Currie, The Behavior of Solder Pastes in Stencil Printing With Vibrating Squeegee, IEEE Transactions on Components, Packaging, Manufacturing Technology, Vol. 21, No. 4, Oct. 1998, pp. 317-324

[61] S. C. Richard, The Complete Solder Paste Printing Processes, Surface Mount Technology, Vol. 13, 1999, pp. 6-8

[62] Peter Krippner, Detlef Beer, AOI Testing Position in Comparison, Circuits Assembly, April 2004, pp. 26-32

[63] David P. Prince, Bridge Detection in the Solder Paste Print Process, 1st January 2006, http://www.speedlinetech.com/docs/Bridge-Detection-Solder-Paste.pdf (accessed 12 July 2009)

[64] K. Fauber, S. Johnson, 2D Versus 3D Solder Paste Inspection http://www.agilent.com/see/aoi 2003 (accessed 12 July 2009)

[65] Rita Mohanty, Vatsal Shah, Paul Haugen, Laura Holte, Solder Paste Inspection Technologies: 2D-3D Correlation, Proceedings of the APEX Conference, April 2008

[66] R. R. J. Lathrop, Solder Paste Print Qualification Using Laser Triangulation, IEEE Transactions on Components, Packaging, Manufacturing Technology, Vol. 20, 1997, pp.174-182

[67] Okura, M. Kanai, S. Ogata, T. Takei, H. Takakusagi, Optimization of Solder Paste Printability With Laser Inspection Technique, Proceedings ot the IEEE/CPMT International Electronics Manufacturing Technology Symposium, 1997, pp. 361-365

[68] E. H. Rideout, Lowering Test Costs With 3-D Solder-Joint Inspection, Test Measurement World, Vol. 10, 1990, pp. 744-1657

[69] Y. K. Ryu, H. S. Cho, New Optical Measuring System for Solder Joint Inspection, Optics and Lasers in Engineering, Vol. 26, No. 6, April 1997, pp. 487-514

[70] H. Tsukahara, Y. Nishiyama, F. Takahashi, T. Fuse, M. Ando, T. Nishino, High-Speed 3-D Inspection System For Solder Bumps, Proceedings of SPIE, Vol. 2597, 1995, pp. 168-177

[71] J. L. Horijon, W. D. Amstel, F. C. Couweleer, W. C. Ligthart, Optical System of an Industrial 3-D Laser Scanner for Solder Paste Inspection, Proceedings of SPIE, Vol. 2599, 1995, pp. 162-170

[72] T. Xian, X. Su, Area Modulation Grating for Sinusoidal Structure Illumination on Phase-Measuring Profilometry, Applied Optics, Vol. 40, 2001, pp.1201-1206

[73] Hsu-Nan Yen, Du-Ming Tsai, Jun-Yi Yang, Full-Field 3-D Measurement of Solder Pastes Using LCD-Based Phase Shifting Techniques, IEEE Transactions on Electronics Packaging, Manufacturing, Vol. 29, No. 1, January 2006, pp. 50-57

[74] XinYu Wu, WingKwong Chung, Hang Tong, A New Solder Paste Inspection Device: Design and Algorithm, IEEE International Conference on Robotics and Automation. Roma, Italy, 10-14 April 2007, pp. 680-685

[75] Fang-Chung Yang, Chung-Hsien Kulo, Jein-Jong Wing, Ching-Kun Yang, Reconstructing the 3D Solder Paste Surface Model Using Image Processing and Artificial

Neural Network, IEEE International Conference on Systems, Man and Cybernetics, Vol. 3, 2004, pp. 3051-3056

[76] Feng Zhang, AEWMA Control Chart for Monitoring Variability Sources of Solder Joints Quality, IEEE Transactions on Components and Packaging Technologies, Vol. 29, No. 1, March 2006, pp. 80-88

[77] Xinyu Wu, Wing Kwong Chung, Jun Cheng, Hang Tong, Yangsheng Xu, A Parallel-Structure Solder Paste Inspection System, IEEE/ASME Transactions on Mechatronics, Vol. 14, No. 5, October 2009, pp. 590-597

[78] CyberOptics SE 300 Ultra, Data Sheet, 8009067, Rev E 1/08

[79] CyberOptics SE 500 Solder Paste Inspection System, Data Sheet, 8013863, Rev A 3/09

[80] Koh Young Technology aSPIre, Data Sheet, aSPIre-B-08-2008-E

[81] Koh Young Technology KY-8030 Series, Data Sheet, KY-8030-B-08-2008-E

[82] Marantz Power Spector SPI Series, 5D Solder Paste Inspection System, Data Sheet, Printed October, 2009, Updated November, 2009

[83] Omron VT-RNS-P, VT-RNS Series, Automated Optical Inspection System, Data Sheet, Printed in Japan, 0807-5M (1004) (D)

[84] Omron CKD VP5000L, Solder Printing Inspection Machine, Data Sheet, Printed July, 2007

[85] Saki BF-SPIder, 3D In-Line Solder Paste Inspection System, Data Sheet, Printed August 2009, PM01DCF01-08.5E

[86] TRI Innovation TR7006 Series, 3D Solder Paste Inspection System, Data Sheet, Updated November, 2008, C-7006-EN-0810

[87] ScanCAD ScanINSPECT SPI, Solder Paste Inspection, Data Sheet, Updated January, 2007

[88] TRI Innovation TR7066 Series, 3D Solder Paste Inspection System, Data Sheet, Updated November, 2009, C-7066-EN-0909

[89] Viscom S3088-II QS, Data Sheet, Updated February, 2009, Viscom_SYS_S3088-II QS_EN09020001

[90] ViTechnology 3D-SPI, Data Sheet, 3D-SPI EN Rev 0507-2009

[91] Michael E. Zervakis, Stefanos K. Goumas, George A. Rovithakis, A Bayesian Framework for Multilead SMD Post-Placement Quality Inspection, IEEE Transactions on Systems, Man and Cybernetics - Part B, Vol. 34, No. 1, February 2004, pp. 440-453

[92] Gao Hongxia, Hu Yueming, Liu Haiming, Fang Xiaosheng, A Fast Method for Detecting and Locating BGA Based on Twice Grading and Linking Technique, 22nd

IEEE International Symposium on Intelligent Control Part of IEEE Multi-conference on Systems and Control Singapore, 1-3 October 2007, pp. 375-378

[93] Bernard C. Jiang, Szu-Lang Tasi, Chien-Chih Wang, Machine Vision-Based Gray Relational Theory Applied to IC Marking Inspection, IEEE Transactions on Semiconductor Manufacturing, Vol. 15, No. 4, November 2002

[94] John Weisgerber, Doreen Tan, Pre-Reflow, Inline, 3-D Inspection, Circuits Assembly, November 2003, pp. 34-36

[95] Chun-Ho Wu, Da-Zhi Wang, Andrew Ip, Ding-Wei Wang, Ching-Yuen Chan, Hong-Feng Wan, A Particle Swarm Optimization Approach for Components Placement Inspection on Printed Circuit Boards, Journal of Intelligent Manufacturing, 2008, DOI 10.1007/s10845-008-0140-2

[96] L. Shih-Chieh, C. Chih-Hsien, S. Chia-Hsin, A Development of Visual Inspection System for Surface Mounted Devices on Printed Circuit Board, Proceedings of the 33rd Annual Conference of the IEEE Industrial Electronics Society (IECON), Taipei, Taiwan, 2007, pp. 2440-2445

[97] A. J. Crispin, V. Rankov, Automated Inspection of PCB Components Using a Genetic Algorithm Template-Matching Approach, The International Journal of Advanced Manufacturing Technology, Vol. 35, No. 3-4, December 2007, pp. 293-300

[98] E. Guerra, J.R.Villalobos, A Three-Dimensional Automated Visual Inspection System for SMT Assembly, Computer and Industrial Engineering, Vol. 40, 2001, pp. 175-190

[99] BeamWorks Inspector cpv, An In-Line AOI System from BeamWorks, Data Sheet, Updated April, 2002

[100] Landrex Optima II 7301 Express, Data Sheet, Updated July, 2006

[101] Omron VT-RNS-Z, VT-RNS Series, Automated Optical Inspection System, Data Sheet, Printed in Japan, 0807-5M (1004) (D)

[102] Viscom S3054QV, Data Sheet, Updated May, 2006

[103] Hongwei Xie, Yongcong Kuang, Xianmin Zhang, A High Speed AOI Algorithm for Chip Component Based on Image Difference, International Conference on Information and Automation, Zhuhai/Macau, China, 22-25 June, 2009, pp. 969-974

[104] G. Acciani, G. Brunetti, G. Fornarelli, A Multiple Neural Network System to Classify Solder Joints on Integrated Circuits, International Journal of Computational Intelligence Research, Vol. 2, No. 4, 2006, pp. 337-348

[105] Y. K. Ryu, H. S. Cho, A Neural Network Approach to Extended Gaussian Image Based Solder Joint Inspection, Mechatronics, Vol. 7, No. 2, 1997, pp. 159-184

[106] Fan-Hui Kong, A New Method for Locating Solder Joint Based On Rough Set, Proceedings of the Sixth International Conference on Machine Learning and Cybernetics, Hong Kong, 19-22 August 2007, pp. 3678-3681

[107] Fan-Hui Kong, A New Method of Inspection Based on Shape from Shading, Congress on Image and Signal Processing, 2008, pp. 291-294

[108] Giuseppe Acciani, Gioacchino Brunetti, Girolamo Fornarelli, Application of Neural Networks in Optical Inspection and Classification of Solder Joints, Surface Mount Technology, IEEE Transasctions on Industrial Informatics, Vol. 2, No. 3, 2006, pp. 200-209

[109] N.S.S. Mar, C. Fookes, P.K.D.V. Yarlagadda, Design of Automatic Vision-Based Inspection System for Solder Joint Segmentation, Journal of Achievements in Materials and Manufacturing Engineering Vol. 34. Issue 2, 2009, pp. 145-151

[110] Da-Zhi Wang, Chun-Ho Wu, Andrew Ip, Ching-Yuen Chan, Ding-Wei Wang, Fast Multi-Template Matching Using a Particle Swarm Optimization Algorithm for PCB Inspection, Lecture Notes in Computer, No. 4974, 2008, pp. 365-370

[111] Hugo C. Garcia, J. René Villalobos, George C. Runger, An Automated Feature Selection Method for Visual Inspection Systems, IEEE Transactions on Automation Science and Engineering, Vol. 3, No. 4, 2006, pp. 394-406

[112] Y. K. Ryu, H. S. Cho, New Optical Measuring System for Solder Joint Inspection, Optics and Lasers in Engineering, Vol. 26, 1997, pp. 487-514

[113] Huibin Zhao, Jun Cheng Jianxun Jin, NI Vision Based Automatic Optical Inspection (AOI) for Surface Mount Devices: Devices and Method, Proceedings of 2009 IEEE International Conference on Applied Superconductivity and Electromagnetic Devices Chengdu, China, 25-27 September 2009, pp. 356-360

[114] Horng-Hai Loh, Ming-Sing Lu, Printed Circuit Board Inspection Using Image Analysis, IEEE Transactions on Industry Applications, Vol. 35, No. 2, March/April 1999, pp. 673-677

[115] Shao-Nung Chiu, Ming-Hwei Perng, Reflection-Area-Based Feature Descriptor for Solder Joint Inspection, Machine Vision and Applications, Vol. 18, 2007, pp. 95–106

[116] Li Ni, Pan Kai-Lin, Li Peng, Research on Solder Joint Intelligent Optical Inspection Analysis, 2008 International Conference on Electronic Packaging Technology & High Density Packaging (ICEPT-HDP), 28-31 July 2008, pp. 1-4

[117] Kuk Won Ko, Hyung Suck Cho, Solder Joints Inspection Using a Neural Network and Fuzzy Rule-Based Classification Method, IEEE Transactions On Electronics Packaging Manufacturing, Vol. 23, No. 2, April 2000, pp. 93-103

[118] Andy Yates, Steven Brown, Jim Hauss, Paul Hudec, Inspection Strategies for 0201 Components, CyberOptics Corporation 2002, First Published: SMTA International, Chicago 2002

[119] T. Y. Ong, Z. Samad, M. M. Ratnam, Solder Joint Inspection With Multi-Angle Imaging and an Artificial Neural Network, The International Journal of Advanced Manufacturing Technology, Vol. 38, No. 5-6, August 2008, pp. 455-462

[120] Y. Ousten, S. Mejdi, A. Fenech, J.Y. Deletage, L. Bechou, M.G. Perichaud, Y. Danto, The Use of Impedance Spectroscopy, SEM and SAM Imaging for Early Detection of Failure in SMT Assemblies, Microelectronics Reliability, Vol. 38, Issue 10, October 1998, pp. 1539-1545

[121] T.H.Kim, T.H.Cho, Y.S.Moon, S.H.Park, Visual Inspection System for the Classification of Solder Joints, Pattern Recognition, Vol. 32, No. 4, 1999, pp. 565-575

[122] T. Hiroi, K. Yoshimura, T. Ninomiya, T. Hamada, Y. Nakagawa, Development of Solder Joint Inspection Method Using Air Stimulation Speckle Vibration Detection Method and Fluorescence Detection Method, IAPR Workshop on Machine Vision Applications, Tokyo, 7-9 December 1992, pp. 429-434

[123] R. Vanzetti, A. C. Traub, A. A. Richard, Automated Laser Inspection of Solder Joints, ISTFA, 1981, pp.85-96

[124] Z.S. Lee, R.C. Lo, Application of Vision Image Cooperated With Multi-Light Sources o Recognition of Solder Joints For PCB, TAAI, Artificial Intelligence and Applications, 2002, pp. 425-430

[125] B. C. Jiang, C.C. Wang, Y.N. Hsu, Machine Vision and Background Remover-Based Approach for PCB Solder Joints Inspection, International Journal of Production Research, Vol. 45, No. 2, 2007, pp. 451-464

[126] J.H. Kim, H.S. Cho, S. Kim, Pattern Classification of Solder Joint Images Using a Correlation Neural Network, Engineering Applications of Artificial Intelligence, Vol. 9, No. 6, 1996, pp. 655-669

[127] T.H. Kim, T.H. Cho, Y.S. Moon, S.H. Park, Visual Inspection System For The Classification of Solder Joints, Pattern Recognition Vol. 324, 1999, pp. 565-575

[128] J.H. Kim, H.S. Cho, Neural Network-Based Inspection of Solder Joints Using a Circular Illumination, Image and Vision Computing, Vol. 13, No. 6, 1995, pp. 479-490

[129] K.W. Ko, H.S. Cho, Solder Joints Inspection Using a Neural Network and Fuzzy Rule-Based Classification Method, IEEE Transactions on Electronics Packaging Manufacturing, Vol. 23, No. 2, 2000, pp. 93-103

[130] T.S. Yun, K.J. Sim, H.J. Kim, Support Vector Machine-Based Inspection of Solder Joints Using Circular Illumination, Electronics Letters Vol. 36, No. 11, 2000, pp. 949-951

[131] D.W. Capson, S.K. Eng, A Tiered-Color Illumination Approach for Machine Inspection of Solder Joints, IEEE Transactions on Pattern Analysis and Machine Intelligence Vo. 10, No. 3, 1988, pp. 387-393

[132] J. H. Kim, H. S. Cho, S. Kim, Pattern Classification of Solder Joint Images Using a Correlation Neural Network, Engineering Applications of Artificial Intelligence, Vol. 9, No. 6, 1996, pp. 655-669

[133] Tae-Hyeon Kim, Tai-Hoon Cho, Young Shik Moon, Sung Han Park, Visual Inspection System for the Classification of Solder Joints, Pattern Recognition Vol. 32, 1999, pp. 565-575

[134] TRI Innovation 7530 Series, Automated Optical Inspection System, Data Sheet, Updated September, 2009, C-7530-EN-0909

[135] Viscom S3016, Data Sheet, Updated Marc, 2007, VISCOM_SYS_S3016_EN06100001

[136] Viscom S3054QC, Data Sheet, Updated June, 2007, VISCOM_SYS_S3054QC_EN06050002

[137] S. Jagannathan, Automatic Inspection of Wave Soldered Joints Using Neural Networks, Journal of Manufacturing Systems, Vol. 16, Issue 6, 1997, pp. 389-398

[138] K. Sundaraj, Homogeneous Pin-Through-Hole Component Inspection Using Fringe Tracking, WSEAS Transactions on Signal Processing, Vol. 4, Issue 7, July 2008, pp. 419-429

[139] F. Wu, X. Zhang, Y. Kuan, Z. Z. He, An AOI Algorithm for PCB Based on Feature Extraction Inspection, Proceedings of the 7th World Congress on Intelligent Control and Automation, Chongqing, China, 25-27 June 2008, pp. 240-247

[140] Machine Vision Products AutoInspector Series - Supra E, Data Sheet, Updated May, 2009

[141] Marantz iSpector HDL Series, In-Line Automatic Optical Inspection Systems, Data Sheet, Printed September, 2009

[142] Marantz iSpector HML Series, In-Line Automatic Optical Inspection Systems, Data Sheet, Printed September, 2009

[143] Saki BF-Tristar, Simultaneous High Speed Inspection for Both Sides of PCB Automated Optical Inspection System, Data Sheet, Printed August, 2009, SJ08DCF01-02.5E

[144] Sony SI-V200, PWB Visual Inspection Machine, Data Sheet, Updated May, 2007, 043E-0705-05-01

[145] TRI Innovation TR7500 Series, Automated Optical Inspection System, Data Sheet, Updated May, 2009, C-7500-EN-0905

[146] TRI Innovation TR7550 Series, Automated Optical Inspection System, Data Sheet, Updated October, 2009, C-7550-EN-0910

[147] Agilent Medalist SJ50 Series 3, Automated Optical Inspection (AOI) and Measurement, Data Sheet, Printed in the USA September, 2006, Updated December 26, 2006 5989-5518EN

[148] Agilent Medalist sj5000, Automated Optical Inspection Solution, Data Sheet, Printed in the USA April, 2008, 5989-7547EN

[149] Amistar Auomation Inc. K2/K2L Optical Circuit Card Inspector, Data Sheet, Updated November, 2008

[150] CyberOptics Flex HR AOI System, Data Sheet, 8013862, Rev A 3/09

[151] Machine Vision Products AutoInspector Series – Ultra IV, Data Sheet, Updated Marc, 2009

[152] Omron VT-RNS-S, VT-RNS Series, Automated Optical Inspection System, Data Sheet, Printed in Japan, 0807-5M (1004) (D)

[153] Omron VT-WIN II, Printed Circuit Board Inspection System, Data Sheet, Printed in the USA 2002

[154] Saki BF-Frontier, Inline High Resolution, High Speed Automated Optical Inspection System, Data Sheet, Printed August, 2009, SJ16DCF01-02.5E

[155] Saki BF-Planet-X, Inline High Resolution, High Speed Automated Optical Inspection System, Data Sheet, Printed August, 2009, SJ06DCF01-02.5E

[156] Viscom S3088-III, Data Sheet, Updated October, 2009, Viscom_SYS_S3088-III_EN09100001

[157] Viscom S3088-II, Data Sheet, Updated August, 2008, Viscom_SYS_S3088-II_EN08080003

[158] Viscom S6056, Data Sheet, Updated July, 2009, Viscom_SYS_S6056_EN09070007

[159] ViTechnology 3K Series, AOI/AOM Systems, Data Sheet, 3K Series EN Rev 04 07-2009

[160] ViTechnology 5K Series, AOI/AOM Systems, Data Sheet, 5K Series EN Rev 03 08-2009

[161] ViTechnology 7K Series, AOI/AOM Systems, Data Sheet, 7K Series CH Rev 02 08-2009

[162] ViTechnology Vi-5000 Series, AOM Systems, Data Sheet, Vi-5000 Series EN Rev 03 01-2008

[163] YES Tech YTV F1 Series, Automated PCB Inspection, Data Sheet, Updated November, 2005

[164] YES Tech YTV M1 Series, Automated PCB Inspection, Data Sheet, Updated Marc, 2009

[165] Egidijus Paliulis, Raimondas Zemblys, Gintautas Daunys, Image Analysis Problems in AOI Systems, Information Technology and Control, Vol. 37, No. 3, 2008, pp. 220-226

[166] Stig Oresjo, Thorsten Niermeyer, Stacy Johnson, Putting Pb-Free to the Test, Circuits Assembly, May. 2005, pp. 42

[167] Detlef Beer, AOI In The Lead-Free Age, OnBoard Technology, June 2005, pp. 36-38

[168] Detlef Beer, Lead-Free: AOI in High-Volume Production Assemblies, Surface Mount Technology, January 2006, pp. 40-41

[169] Thorsten Niermeyer, Controlling Pb-Free Processes Through AOI, Circuits Assembly, October 2004, pp. 40-41

[170] Paul R. Groome, Lead-Free, PCB Test and Inspection, Surface Mount Technology, November 2005, pp. 36-39

[171] Shu Peng, Sam Wong TS, Test Implications of Lead-Free Implementation in a High-Volume Manufacturing Environment, Proceedings of the International Test Conference (ITC), 8-8 November 2005, pp. 620-627

[172] Paul R. Groome, Lead-Free: PCB Test and Inspection, Surface Mount Technology, 1 November 2005, pp. 36-39

[173] Jim Fishburn, Advances in Lead-Free Soldering and Automatic Inspection, Surface Mount Technology, November 2002, pp. 46-47

[174] Du-Ming Tsai, Cheng-Hsiang Yang, A Quantile–Quantile Plot Based Pattern Matching for Defect Detection, Pattern Recognition Letters, No. 26, 2005, pp. 1948-1962

[175] Ahmed Nabil Belbachir, Mario Lera, Alessandra Fanni, Augusto Montisci, An Automatic Optical Inspection System for the Diagnosis of Printed Circuits Based on Neural Networks, Proceedings of the Industry Applications Conference, 2005, pp. 680-684

[176] Immanuel Edinbarough, Roberto Balderas, Subhash Bose, A Vision and Robot Based On-Line Inspection Monitoring System for Electronic Manufacturing, Computers in Industry, No. 56, 2005, pp. 986-996

[177] Du-Ming Tsai, Chien-Ta Lin, Fast Normalized Cross Correlation for Defect Detection, Pattern Recognition Letters No. 24, 2003, pp. 2625-2631

[178] Chiu-Hui Chen, Chun-Chieh Wang, Chun-Yu Lin, Yu-Sen Shih, Chung-Fan Tu, Realization of Defect Automatic Inspection System for Flexible Printed Circuit (FPC), Proceedings of the 35th International MATADOR Conference, 2007, pp. 225-228

[179] Sean P. Cunningham, Scott MacKinnon, Statistical Methods for Visual Defect Metrology, IEEE Transactions on Semiconductor Manufacturing, Vol. 11, No. 1, February 1998, pp. 48-53

[180] Dr. Kwangli Koh (Koh-Young), Eliminating False Calls With 3D AOI Technology, EPP Europe, Issue 4, 2009, pp. 40-43

[181] Wei-Hung Su, Kebin Shi, Zhiwen Liu, Bo Wang, Karl Reichard, Shizhuo Yin, A Large-Depth-of-Field Projected Fringe Profilometry Using Supercontinuum Light Illumination, Optics Express, Vol. 13, No. 3, February 2007, pp. 1025-1032

[182] Günther Wernicke, Matthias Dürr, Hartmut Gruber, Andreas Hermerschmidt, Sven Krüger, Andreas Langner, High Resolution Optical Reconstruction of Digital Holograms, Fringe 2005, Session 4, 2005 pp. 480-487

[183] Liu Xiao-Li, Li A-Meng, Zhao Xiao-Bo, Gao Peng-Dong, Tian Jin-Dong, Peng Xiang, Model-Based Optical Metrology and Visualization of 3-D Complex Objects, Optoelectronics Letters, Vol. 3, No.2, 15 Mar. 2007, pp. 115-118

[184] Marek Wegiel, Malgorzata Kujawinska, Fast 3D Shape Measurement System Based on Color Structure Light Projection, Fringe 2005, Session 3, 2005, pp. 450-453

[185] Simon Davis, Lead-Free Inspection And Qualification With 3D AOI, OnBoard Technology November 2005, pp. 54-57

[186] Zulki Khan, A Primer on AOI and AOT, Circuits Assembly, September 2006, pp. 38-41

[187] Dongwon Shin, Thomas R. Kurfess, Three-Dimensional Metrology of Surface Extracted From a Cloud of Easured Points Using a New Point-to-Surface Assignment Method: An Application to PCB-Mounted Solder Pastes, Precision Engineering Vol. 28, Issue 3, July 2004, pp. 302-313

[188] Tae-Hyeon Kim, Tai-Hoon Cho, Young Shik Moon, Sung Han Park, An Automated Visual Inspection of Solder Joints Using 2D and 3D Features, Proceedings on the 3rd IEEE Workshop on Applications of Computer Vision, 1996. pp. 110-115

[189] Deokhwa Hong, Hyunki Lee, Min Young Kim, Hyungsuck Cho, Jeon Il Moon, Sensor Fusion of Phase Measuring Profilometry and Stereo Vision for Three-Dimensional Inspection of Electronic Components Assembled on Printed Circuit Boards, Applied Optics, Vol. 48, No. 21, 20 July 2009, pp. 4158-4169

[190] S. S. Wong, K. L. Chan, 3D Object Model Reconstruction From Image Sequence Based on Photometric Consistency in Volume Space, Pattern Analysis and Application, November 2009, DOI 10.1007/s10044-009-0173

[191] Deokhwa Hong, Heechan Park, Hyungsuck Cho: Design of a Multi-Screen Deflectometer for Shape Measurement of Solder Joints on a PCB, Proceedings of the IEEE International Symposium on Industrial Electronics (ISIE), 2009, pp 127-132

[192] Jiquan Ma, Solder Joint's Surface Recovery Based on Linear Hybrid Shape-From-Shading, Proceedings of the Second Asia-Pacific Conference on Computational Intelligence and Industrial Applications (PACIIA), 2009, pp. 245-249

[193] Akira Kusano, Takashi Watanabe, Takuma Funahashi, Takayuki Fujiwara, Hiroyasu Koshimizu, 3D Inspection of Electronic Devices by Means of Stereo Method on Single Camera Environment, Proceedings of the Industrial Electronics (IECON), 2008, pp. 3391-3396

[194] Sheng Liu, Dathan Erdahl, I. Charles Ume, Achyuta Achari, Juergen Gamalski, A Novel Approach for Flip Chip Solder Joint Quality Inspection: Laser Ultrasound and Interferometric System, IEEE Transactions On Components and Packaging Technologies, Vol. 24, No. 4, December 2001, pp 616-624

[195] Grantham K.H. Pang, Ming-Hei Chu, Automated Optical Inspection of Solder Paste based on 2.5D Visual Images, Proceedings of the IEEE International Conference on Mechatronics and Automation, 2009, pp 982-987

[196] Atsushi Teramoto, Takayuki Murakoshi, Masatoshi Tsuzaka, Hiroshi Fujit, Automated Solder Inspection Technique for BGA-Mounted Substrates by Means of Oblique Computed Tomography, IEEE Transactions on Electronics Packaging Manufacturing, Vol. 30, No. 4, October 2007, pp. 285-292

[197] Jun Cheng, Chi-Kit Ronald Chung, Edmund Y. Lam, Kenneth S. M. Fung, Fan Wang, W. H. Leung, Structured-Light Based Sensing Using a Single Fixed Fringe Grating: Fringe Boundary Detection and 3-D Reconstruction, IEEE Transactions on Electronics Packaging Manufacturing, Vol. 31, No. 1, January 2008, pp. 19-31

[198] Yunxia Gao, Jun Wang, Testing Failure of Solder-Joints by ESPI on Board-Level Surface Mount Devices, Proceeding of the International Conference on Electronic Packaging Technology & High Density Packaging (ICEPT-HDP), 2009, pp. 1256-1259

INTECH

INTECH

INTECH